ISASINDIA Newsletter

Vol 21, No. 2 *April 2021*

From Editor's Desk

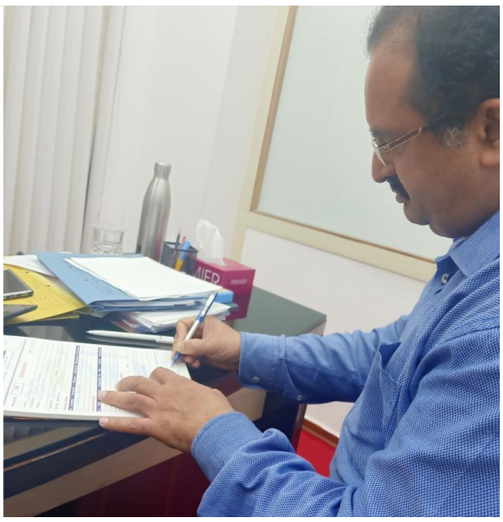

Dear ISAS Members

I warmly welcome all of you on this issue of ISAS newsletter.

Unfortunately India is facing second wave of CORONA . We pray almighty to help India in this crucial time of pandemic. Scientific community has a vital role to play in association with Indian Government. ISAS has kept its activities going on by means of arranging online activities such as conducting internet lectures through zoom.

In hospitals difficulty is being faced in procuring uninterrupted supply of Oxygen which is life saving for Covid patients. ISAS president has written letter to prime minister Narendra Modi persuading to launch a Massive National Mission To Generate & Preserve Greenery. Thus ISAS is working on many fronts. Article " Carbon based materials for nuclear applications" by Shanti Swarup Bhatnagar awardee has been included.

An articles entitled "Supercritical Fluid Extraction of Uranium from Aqueous and Solid Matrix" by Dr. Pradeep Kumar, Vice president of ISAS provides elegant knowledge in frontier area of separation science and technology. The Nobel Prize in Chemistry 2020 was awarded jointly to Emmanuelle Charpentier and Jennifer A. Doudna "for the development of a method for genome editing." Their work has been compiled in an article. Articles "Design and development of Optics for High Energy, High Power Nd:glass Lasers" by A.S. JOSHI has been included.

Take care of yourself and family, protecting yourself from prevailing Pandemic situation.

Suggestions by viewers are most welcome.

Dr. Pradeep Kumar

Vice President , ISAS

Chief Editor of ISAS,

Message From President, ISAS

****

Our Nation is currently undergoing a trying situation due to the menacingly massive second wave of Covid.

It is a matter of great satisfaction to note that the scientific community, of BARC and DAE, is contributing significantly to the management of Covid Pandemic, in terms of radiation stertilisation of PPEs, High Efficiency Masks, Oxygen Generators, etc

This is the time for our scientific community to come forward, to contribute to "Aatma Nirbharata Ptogrammes" and, also, actively disseminate scientific information reaching out to the common man through the umpteen intermediary linkages such as academicians, working and retired scientists and technologists, etc.

ISAS is happy that we, the ISAS Technical Team, are doing it very well through the every-week-end ISAS Webinars, incessantly.

Looking forward to, the sooner day, when our great Motherland comes out inbflying colours, like The Phoenix, As An Ever Youthful and Strong World Leader in Science, Technology and Unifying Spirituality Of Bhaarat Varsham.

Best Wishes To The ISAS Fraternity.

Jai Maharashtra.

Jai Hind.

****

Carbon based Materials for Nuclear Applications

Kinshuk Dasgupta

Materials Group, Bhabha Atomic Research Centre

Mumbai 400085, India

Dr. Kinshuk Dasgupta,
Head Advanced Carbon Materials Section
and AMD Material Group, BARC , Mumbai.
Shanti Swarup Bhatnagar awardee

Carbon is a wonderful material with wide range of structures and properties. It can have crystalline (such as, graphite, diamond, carbon nanotube) as well as disordered (such as, carbon black, glassy carbon) structures. The bonding in carbon materials may vary from sp^2 to sp^3 hybridization.Carbon materials possess capability to withstand high temperature (in protective environment), increased strength up to 2500^0C, chemical inertness, low coefficient of thermal expansion, good thermal conductivities, low density and good thermal shock resistance. Carbon nanomaterials have very high specific surface area, useful for adsorptive separation. The versatilities of carbon materials have made them useful for various structural and functional applications in nuclear field.

Graphite is widely used in nuclear applications. The first nuclear reactor CP-1, constructed in 1942 at Stagg Field University of Chicago used graphite as the moderator [1]. Graphite has very high thermal shock resistance and its creep rate is very small below 1500°C. The tensile strength of graphite increases with temperature and is about twice at 2500°C as against the room temperature. Graphite does not melt but sublimes at 3650°C. The low atomic weight with high neutron scattering probability and stability under irradiation has made graphite a right choice for moderator in high temperature reactors. Advanced gas cooled reactor (AGR), the high temperature gas-cooled reactors (HTGR), the molten salt breeder reactors (MSBR) and the liquid metal-fuelled reactors (LMFR) all use graphite moderators [1]. Indian High Temperature Reactor (IHTR) design uses graphite as the reflector [2]. Figure 1 shows some prototype graphite components for IHTR. Indian research reactor CIRUS also used graphite as the reflector.

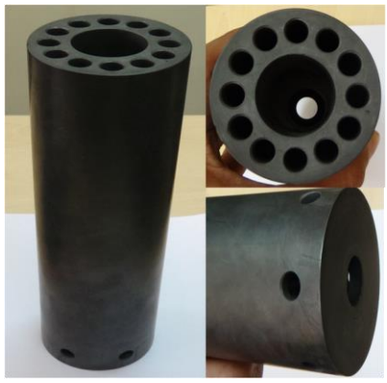

Figure 1: Prototype graphite components for IHTR

The main function of graphite as the moderator and the reflector is to reduce the kinetic energy of the fast neutrons released at fission. Fast neutrons have energies of the order of 2MeV. However, neutrons having thermal energies of the order of 0.025 to 0.1 eV are ideal for sustaining the fission reaction. The moderation process happens by repeated elastic collisions of the neutrons with the nuclei of the moderator material. The smaller the mass of the moderator nucleus the larger is the transferred energy, which attains its maximum value when the moderator nucleus has the same mass as that of the neutron. If the energy of the recoil (knock-on) nucleus of the moderator is sufficient to permit it to be displaced from its equilibrium position in the space lattice, physical changes may be observed. As a general rule, the primary knock-on atom acquires sufficient kinetic energy to displace another atom by collision and the latter becomes a secondary knock-on. The process continues until the displaced atom does not have sufficient energy to eject another atom from the equilibrium position [3]. When carbon-based materials are used in nuclear reactors their properties change due to irradiation damage. Graphite in particular tends to accumulate energy due to lattice displacementof carbon atoms by energetic particles such as neutrons. The stored energy is known as Wigner energy [4]. The energy stored in graphite under irradiation at ambient temperature is around 2700 J/g which when released adiabatically would cause its temperature to rise to 1300°C. In order to reduce or limit the stored energy it is essential to anneal the irradiated graphite. However, it is noted that stored energy ceases to be a problem at temperature of irradiation above 300°C. Figure2shows the stored energy release curves of graphite irradiated at 30^0C in the Handford K reactor cooled test hole [5]. To avoid this, graphite has to be annealed frequently to remove the stored energy. In high temperature nuclear reactors graphitic carbon is theunanimous choice as the moderator material, where thesedefects get annealed due to high temperature. However, for thelow temperature thermal reactors like Advanced Heavy Water Reactor (AHWR) [6], accumulation of Wigner energy and its sudden release may

be a problem for graphite and therefore, amorphous carbon composite is a better choice over graphite [7,8].

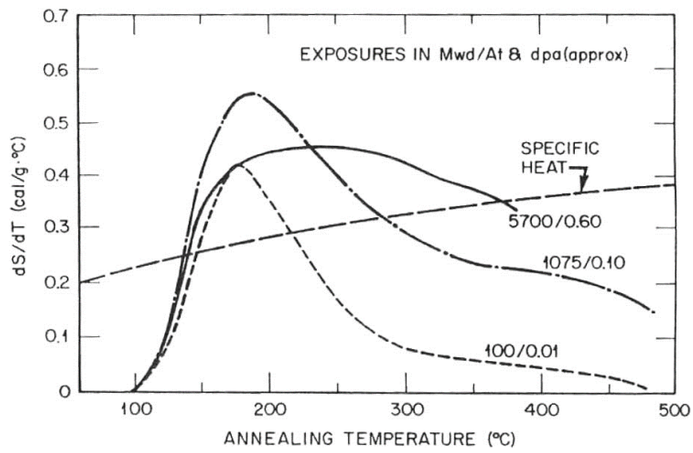

Figure 2: Stored energy release curves of graphite irradiated at 30^0 C in the Handford K reactor cooled test hole [5]

Apart from moderator application, carbon finds usein a control rod material when combined with some forms of boron or other high neutron absorbing elements [9] of high temperature stability. Graphite also serves as a stable matrix because it is able to withstand localized alpha recoil damage, offering protection against gross shield degradation. In combination with components of U or Th, graphite offers advantages as a matrix for fissile or fertile reactor fuel in thermal reactors [10]. Here graphite serves dual purpose as a moderator and stable disbursing phase of fuel. Graphite also offers an exceptional heat transfer medium for heat removal and resists thermal shock.

In high temperature reactors, purified artificial graphite is used as a structural material for the fuel element. There are two basic designs of fuel elements: the pebble bed and the prismatic core [11]. In the pebble bed reactor, the core is made up of randomly packed spheres of 60 mm while the prismatic design is made up of stacked machined or pressed graphite stacks which also incorporates coolant channels and separate holes for fuel.

A high temperature reactor contains spherical coated fuel. An individual particle consists of a kernel of fissile or fertile fuel surrounded by number of layers, which are designed to retain the fission products that are formed during the course of irradiation. The fuels may be oxides, carbides or mixed oxide/carbide forms of uranium, plutonium or thorium. Two distinct particle designs have been employed namely the BISO (Bi-isotropic) coated and the TRISO (Tri-isotropic) coated fuel [10,12]. The BISO coated particles possess two layers, a highly porous pyrocarbon (PyC) coating (buffer layer), which is surrounded by a denser PyC layer. BISO particles have only been employed in fertile fuel particles where there is low irradiation temperature and low burnups. In the TRISO coated particle the kernel is coated by a buffer layer followed by three

successive layers, namely, the inner pyrocarbon (IPyC), SiC layer and an outer pyrocarbon (OPyC) layer (Figure3).

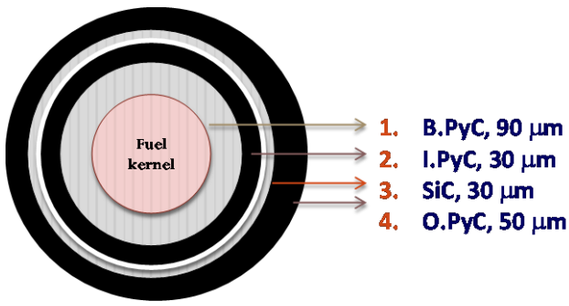

Figure 3: Schematic of a TRISO coated particle

More recently, Pyrolytic graphite, artificial fine-grained graphite and C-C composites have been adopted as plasma facing components in fusion devices [5]. Tokomak fusion devices utilize carbon materials for their first-wall linings, limitor and for armor on their plasma-facing components (PFC) as shown in Figure4. C-C composites possess a number of attributes such as low atomic number, high thermal shock resistance, high sublimation temperature and high thermal conductivity, which makes it a good choice in the fusion reactors. C-C components materials may be the choice for the next generation Tokomak fusion reactors such as International Thermonuclear Experimental Reactor (ITER) which must endure severe environment including high-heat fluxes, high armor, surface temperature and eddy-current induced stresses during plasma disruption. The plasma-facing carbon-carbon composite materials will suffer structure and property degradation as a result of carbon atom displacements and crystal lattice damage, caused by impinging high-energy fusion neutrons and energetic helium ions for carbon transmutations. As C-C composites are infinitely variable family of materials, the processing and design variables such as; (1) architecture, i.e., 1D, 2D, 3D or random fiber distribution; (2) fiber precursor, i.e., pitch, polyacrylonitrile (PAN) or vapour grown; (3) matrix, i.e., liquid impregnation (pitch or resin) or CVI; and (4) final graphitisation temperature will influence the properties and behaviour of C-C composites. Burchell et al. [10] irradiated 1D, 2D, and 3D C-C composites at 600°C and to damage doses upto 1.5dpa. 3D C-C composites were shown to have more isotropic dimensional changes than that of 1D or 2D composites. Pitch fiber composites were shown to be more dimensionally stable than PAN fiber composites and high graphitisation temperatures were found to be beneficial.

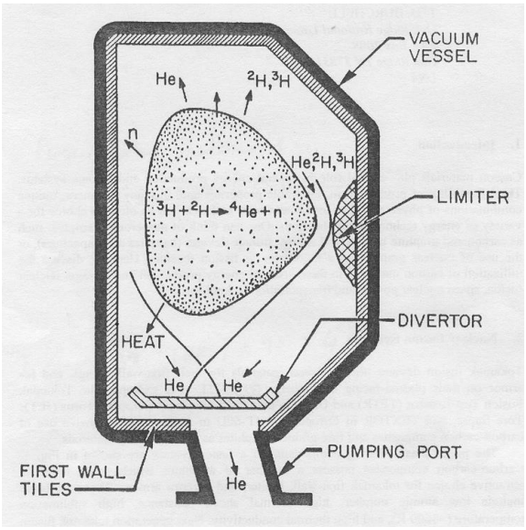

Figure 4: Schematic of the plasma-facing components of a Tokomak fusion reactor [5]

In recent times carbon nanotube (CNT) and graphene find applications in front-end and back-end of nuclear fuel cycles. Extractant encapsulated CNT-PVA composite beads (Figure 5) have been utilized for rare-earth extraction [13,14]. The CNT addition improves the extraction capacity and the rate of extraction several times. Functionalized CNT has been used for recovery of Nd metal ions from magnetic scrap [15] (Figure 6).

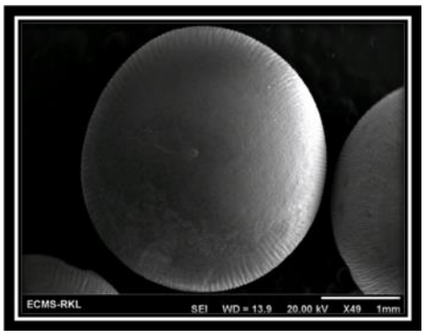

Figure 5: Typical CNT-PVA beads

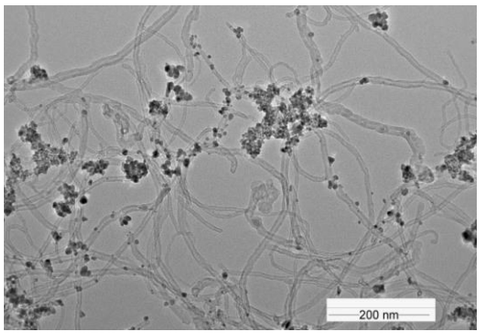

Figure 6: Nd metals attached to CNTs [15]

Functionalized graphene and carbon nanotubes have been extensively used for the actinide separation from high level radioactive wastes [16-18]. Both theoretical studies and practical experiments suggest that task specific functionalization of carbon nanomaterials is helpful for selective adsorption of lanthanides and actinides onto the surface of the nanomaterials. Nuclear desalination also employs various carbon nanomaterials [19-20].

To summarize, carbon based materials starting from graphite, C-C composite, carbides, carbon coatings to carbon nanomaterials are widely used nuclear industry. This has been possible due to the fact that the structures of carbon can be tailor made depending on the applications.

References:

1. R. E. Nightingale. Graphite in Nuclear Industry. In NuclearGraphite Nightingale RE, editor. New York and London, Academic Press: 1962; p 1-20
2. I.V. Dulera, R.K. Sinha, A. Rama Rao, R. J. Patel. High temperature reactor technology development in India, Prog. Nuclear Energy 101 (2017) 82-99
3. S. Glasstone, and A. Sesonske. Nuclear Reactor Engineering, Fourth edition, Vol. 1, CBS Publishers, New Delhi,India, 1998, Chapter 1&3.
4. R. E. Nightingale. Stored Energy. In Nightingale RE, editor. Nuclear Graphite, New York and London: Academic Press: 1962; p 325-353.
5. Pyrocarbon in high temperature nuclear reactors. Chapter-7. In Irradiation damage in graphite due to fast neutrons in fission and fusion systems, IAEA TECDOC-1154, September 2000, IAEA, Vienna, Austria.
6. R.K. Sinha, A. Kakodkar. Design and development of the AHWR – the Indian thorium fuelled innovative nuclear reactor.Nucl. Eng. Des. 236 (2006) 683–700.
7. K. Dasgupta, J. Prakash, B. M. Tripathy. Novel low Wigner energy amorphous carbon-carbon composite. Journal of Nuclear Materials 445 (2014) 72–77
8. K. Dasgupta, P. Barat, A. Sarkar, P. Mukherjee, D. Sathiyamoorthy. Stored energy release behaviour of disordered carbon.Appl. Phys. A 87, 721–726 (2007)
9. A. K. Suri, C. Subramanian, J. K. Sonber, T. S. R. Ch Murthy. Synthesis and consolidation of boron carbide: A review. International Materials Reviews 55 (2010) 4-40
10. T. D. Burchell. Carbon Materials for Energy productionand Storage. In Design and Control of Structure of AdvancedCarbon Materials for Enhanced Performance. Rand, B. et al., editor. Kluwer Academic Publishers, Dordrecht, Netherlands, **2001**, 277-294.
11. J. Guilleray,R. L. R. Lefevre, M. S. T. Price. Pyrocarbon coating of nuclear fuel particles. In Chemistry and Physics of Carbon, Vol. 15, edited by Walker PL and Thrower PA, New York: Dekker, 1965.
12. R. E. Bullock. Irradiation performance of experimental fuel particles coated with silicon alloyed pyrocarbon: A review. J. Nuclear Materials 1983, 113, 81-150.
13. K. K. Yadav, K. Dasgupta, D. K. Singh, M. Anitha, L. Varshney, H. Singh. Solvent impregnated carbon nanotube embedded polymeric composite beads: An environment benign approach to the separation of rare earths. Separation and Purification Technology 143 (2015) 115-124
14. K. K. Yadav, K. Dasgupta, D. K. Singh, L. Varshney, H. Singh. Dysprosium sorption by polymeric composite bead: Robust parametric optimization using Taguchi method. J Chromatography A 1384 (2015) 37-43
15. K. Dasgupta, R. Vijayalakshmi, M. Anitha. Recovery of Nd(III) in coexistence with Fe(III) ions from aqueous phase using functionalized multiwalled carbon nanotubes: An environmental benign approach. Journal of Environmental Chemical Engineering 4 (2016) 2103-2113
16. A. Singha Deb, S. Pahan, K. Dasgupta, S. Panja, A. K. Debnath, P. S. Dhami, M. Sk. Ali, C. P. Kaushik, J. S. Yadav. Carbon nanotubes functionalized with novel functional group amido-amine for sorption of actinides. Journal of Hazardous Materials 345 (2018) pp 63-75
17. A. Sengupta, A. K. Singha Deb, K. Dasgupta, V. C. Adya, Sk. M. Ali. Diglycolamic acid functionalized multiwalled carbon nanotube highly efficient sorbent for f-block elements: Experimental and theoretical investigation. New Journal of Chemistry 41 (2017) 4531-4545
18. P. Kumar, A. Sengupta, A. Singha Deb, K. Dasgupta, Sk. M. Ali. Sorption behaviour of Pu^{4+} and PuO_2^{2+} on amido amine functionalized Carbon nanotube: Experimental and Computational study. RSC Adv. 6 (2016) 107011-20
19. S. Kar, R. C. Bindal, S. Prabhakar, P. K. Tewari, K. Dasgupta and D. Sathiyamoorthy. Potential of Carbon nanotubes in Water Purification: An Approach towards the Development of an Integrated Membrane System. Int. J. Nuclear Desalination 3 (2008) pp 143-150
20. S. Kar, R. C. Bindal, P. K. Tewari. Carbon nanotube membranes for desalination and water purification: Challenges and opportunities. Nano Today 7 (2012) 385-389

Supercritical Fluid Extraction of Uranium from Aqueous and Solid Matrix

Dr. Pradeep Kumar

Senior Scientist, Bhabha Atomic Research Centre, Trombay

Chief editor and Vice president, ISAS.

The present article describes Author's experience on supercritical fluid extraction of uranium and thorium from aqueous and solid matrix. Extraction and purification of actinides from various matrices is of utmost importance in the nuclear industry. Conventional techniques for the separation and purification of actinides (uranium, thorium, plutonium) from various matrices largely rely on solvent extraction [1]. Large amount of liquid volume comprising of used organic solvents and acids is generated in the conventional solvent extraction process. In the recent years, supercritical fluid extraction (SFE) has emerged as a promising alternative to conventional solvent extraction process owing to its potential to minimize the generation of the radioactive liquid volume and simplification of the extraction process. SCFs have characteristics of liquid as well as gas. Properties of SCF such as density, diffusivity, viscosity and surface tension are intermediate to that of liquid and gas. From extraction point of view, the unique characteristic of SCF is its solvating property. Supercritical fluid extraction process assumes significance as it exhibits practical advantages such as enhanced extraction rate due to rapid mass transfer in supercritical fluid medium and change of solvent properties such as density by tuning pressure / temperature conditions. Supercritical fluids (SCF) offer faster, cleaner and efficient extraction owing to low viscosity, high density, low surface tension and better diffusivity properties. Higher diffusivity than liquids facilitates rapid mass transfer and faster completion of reaction. Due to low viscosity and surface tension, SCF can penetrate deep inside the material, extracting the component of interest. Liquid like solvating characteristics of SCFs enable dissolution of compounds whereas gas like diffusion characteristics provide conditions for high degree of extraction in shorter time duration.

When a gas is compressed to a sufficiently high pressure, it becomes liquid. If, on the other hand, the gas is heated beyond a specific temperature, no amount of compression of the hot gas will cause it to become liquid. This temperature is termed as the critical temperature (T_c) and the corresponding vapor pressure as the critical pressure (P_c). These values of temperature and pressure define critical point, which is unique to a given substance. A substance above critical point is said to exist in the supercritical fluid (SCF) state. CO_2 was selected as supercritical fluid owing to its moderate critical constants (Pc= 72.9 atm, Tc =31.3 ºC, ρ_c = 0.47 g/mL) and attractive properties such as being easily available, recyclable, non-toxic, chemically inert, non inflammable and radio-chemically stable.

Hanny and Hogarth [2] were the first to report the unique solvating properties of supercritical fluids as early as 1879. In 1958, Lovelock [3] suggested the use of SCFs in chromatography. Klesper *et al.* [4] in 1962, demonstrated chromatographic separation of nickel porphyrins using supercritical chlorofluoromethanes as mobile phase. SCFs were employed for extraction and recovery of organic compounds from solid materials [5]. However, direct extraction of metal ions with SC CO_2 is known to be highly inefficient because of the charge neutralization requirement and the weak solute-solvent interactions. For metal ion extraction by SC CO_2 a suggested approach was to form metal complexes with organic complexing agents, those metal-complexes could be soluble in SC CO_2. Wai *et al.* [6] demonstrated the SFE of Cu^{2+} from liquid and solid medium by SC CO_2 containing fluorinated chelating agent. Subsequently, SFE of many metal

ions was reported [7]. Lin *et al.* [8] performed SFE of trivalent lanthanides and uranyl ions from solid material. .

Table-1 Comparison of Physical Properties of Different States

State	Density (g ml^{-1})	Viscosity (poise)	Diffusivity (cm^2 s^{-1})
Gas	10^{-3}	$(0.5\text{-}3.5)*10^{-4}$	0.01-1.0
Supercritical Fluid	0.2-0.9	$(0.2\text{-}1.0)*10^{-3}$	$(3.3\text{-}0.1)*10^{-4}$
Liquid	0.9-1.0	$(0.3\text{-}2.4)*10^{-2}$	$(0.5\text{-}2.0)*10^{-5}$

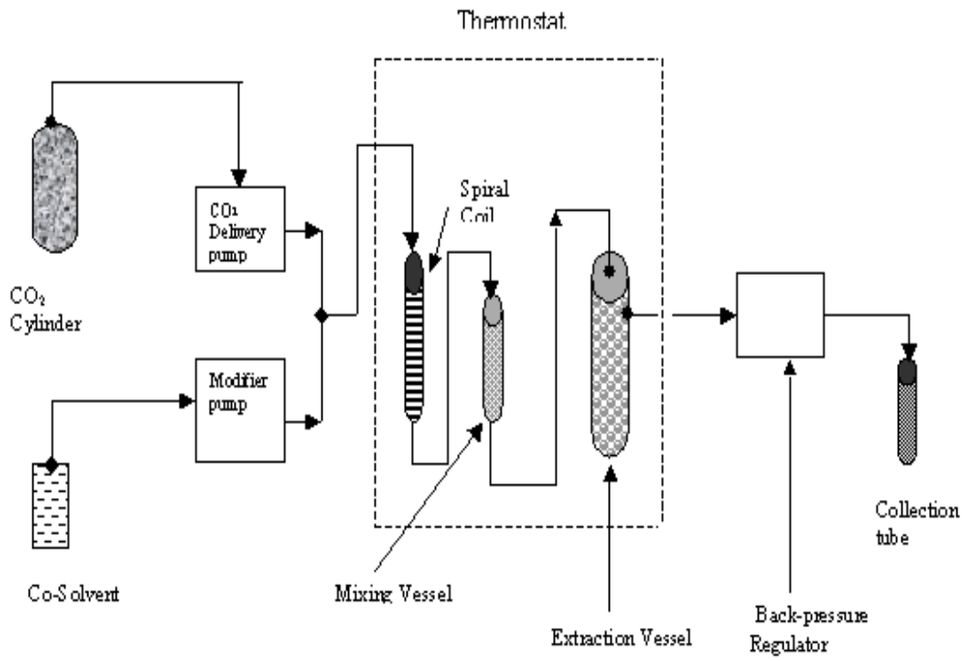

Fig. 1. A schematic diagram of SFE set-up

Experimental set-up

A schematic of supercritical fluid extraction set-up is shown in Fig.1. The supercritical fluid extraction set-up mainly consists of CO_2 delivery pump, modifier pump, thermostat, back-pressure regulator and collection vessel. CO_2 gas from cylinder was fed into the CO_2 delivery pump where it was liquefied to 263 K. The pump supplied liquid CO_2 at desired flow rates. The modifier pump provided the desired co-solvent flow rate. The CO_2 and co-solvent flow rates could be varied from 0.001 to 10 ml min^{-1} with a precision of 0.001 ml min^{-1}. The CO_2 and co-solvent streams were merged into a single stream by a T-joint to produce mixture of CO_2 containing the desired percentage of co-solvent. The stream was then allowed to pass through a 5-meter long spiral coil for thorough mixing of CO_2 and co-solvent. High level of homogeneity was achieved by passing the stream through a 10 mL capacity cylindrical vessel containing spherical teflon pebbles. The stream then entered a six-port valve, which had provision for selecting/ bypassing the extraction vessel. Spiral coil and mixing vessel are contained in the thermostat. The stainless steel extraction vessel (10 mL) were cylindrical in shape. Extraction vessel consists of inlet and outlet at the top. The inlet stainless steel tube (0.5 mm inner diameter), passing through center of extraction vessel from top, extended upto bottom for purging supercritical CO_2 through the sample solution. Back-pressure regulator controlled the pressure of the extraction vessel by means of opening/closing of variable stroke needle valve. Pressure could be varied from atmospheric pressure upto 500 atm with a precision of $\pm$ 1 atm. The

temperature of thermostat could be varied from room temperature upto 353 K with a precision of ± 0.1 K. The extract coming out from the outlet of extraction vessel was collected in a collection tube at atmospheric pressure where CO_2 escaped as gas. Each unit of the set-up can be independently controlled by its inbuilt microprocessor. Additionally, provision exists for controlling all units collectively (except back-pressure regulator) through computer. All the parameters could be set, controlled and monitored by a software programme which can also control CO_2 delivery pump rate, modifier pump rate and temperature of the thermostat.

Theoretical aspects of uranium SFE

A probable extraction scheme for uranium extraction from nitric acid medium into supercritical CO_2 is depicted in Fig.2. Uranium extraction process into supercritical CO_2 involves many equilibria processes. Uranium is extracted as $UO_2(NO_3)_2.2(TBP)$ into supercritical CO_2 phase.

The extraction reaction involves at least three elemental processes: (i) Distribution of TBP between aqueous and supercritical CO_2 phases, (ii) formation of complex $UO_2(NO_3)_2 .2(TBP)$ in the aqueous phase and (iii) distribution of the complex between aqueous and supercritical CO_2 phases. The overall extraction reaction could be expressed by the following formula:

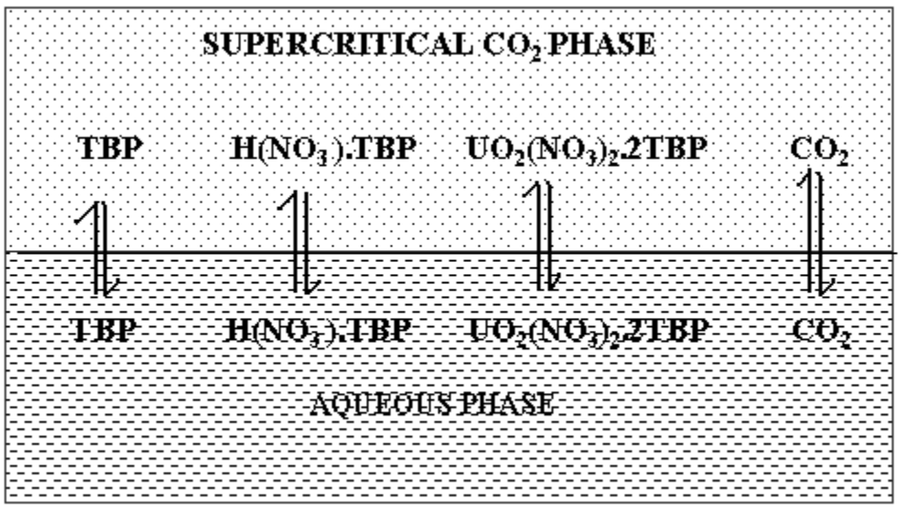

Fig.2. Extraction scheme of UO_2^{2+} from nitric acid into supercritical CO_2 employing TBP as co-solvent

$$UO_2^{2+}{}_{aq} + 2\ TBP_{SF} + 2\ NO^-{}_{3\ aq} \overset{K_{ex}}{\rightleftharpoons} \{UO_2(NO_3)_{2..}2(TBP)\}_{SF} \quad (1)$$

Where, K_{ex} is extraction constant defined by following equation:

$$K_{ex} = \frac{\left[UO_2(NO_3)_2.2(TBP)\right]_{SF}}{\left[UO_2^{2+}\right]_{aq}\left[TBP\right]^2_{SF}\left[NO^-_3\right]^2_{aq}} \quad (2)$$

The uranium distribution ratio and extraction constant are related by Eq.(3).

$$\log D_U = \log K_{D,U-TBP} + \log K_{f,U\text{-}TBP} - 2\log K_{D,TBP} + 2\log[NO_3]_{aq} + 2\log[TBP]_{SF} \quad (3)$$

Where $K_{D,TBP}$ and $K_{D,U\text{-}TBP}$ are the phase distribution constants of TBP and U-TBP complex and $K_{f,U\text{-}TBP}$ is the formation constant of U-TBP complex in the acid solution.

Extraction efficiency depends upon solvating power (solubility) of supercritical CO_2. Chrastil [11] has arrived at a simple empirical correlation relating solubility of the solute 'S' with the density 'ρ'of the supercritical fluid respectively:

$$\ln S = k \ln \rho + C \quad (4)$$

'k' corresponds to the number of CO_2 molecules solvating around the solute molecule and the constant 'C' is a temperature-dependent term consisting of thermal properties such as the solvation heat, vaporization heat and/or the volatility of the solute. The phase distribution constant $K_{Dj\ of}$ substance is related to its solubility and supercritical fluid density by Eq. (5).

$$\log K_{Dj} = k_j \log \rho + C_j - \log S_{j,aq} \quad (5)$$

The above equations are valid for equilibrium system. However, in SFE, supercritical fluid phase is continuously flown, overtly extraction efficiency depends on two basic factors: (i) distribution ratio of metal-complex and (ii) kinetics of transport of metal-complex into supercritical CO_2.

Optimization of parameters

Initially, the SFE of uranium was carried out from acidic medium employing TBP as co-solvent. Various parameters influencing uranium extraction efficiency were identified and systematic study was carried out [12]. Experimental conditions are listed in Table 2.

Table 2. Experimental conditions for parameter study of SFE of uranium from acidic medium with TBP as co-solvent

Uranium concentration	500.8 μg ml^{-1}
Uranium solution in extraction vessel	5 ml
Molarity of uranium solution	4 M
Extraction time	30 minute
Extraction mode	Dynamic
Complexation mode	Online
Collection liquid ($CHCl_3$)	3 ml
CO_2 flow rate	1 ml min^{-1}
TBP flow rate	0.1 ml min^{-1}

Effect of pressure and Temperature on Extraction efficiency

Pressure versus extraction efficiency graph in the 80-300 atm range at 60 ºC displays initial steep rise in extraction efficiency followed by a gradual decline.

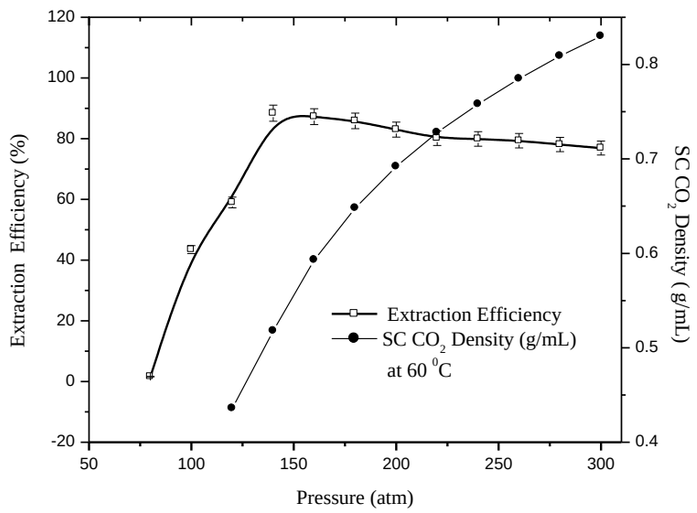

Graph of pressure versus uranium extraction efficiency/ SC CO_2 density
(Error bar is ± 3% of the value)

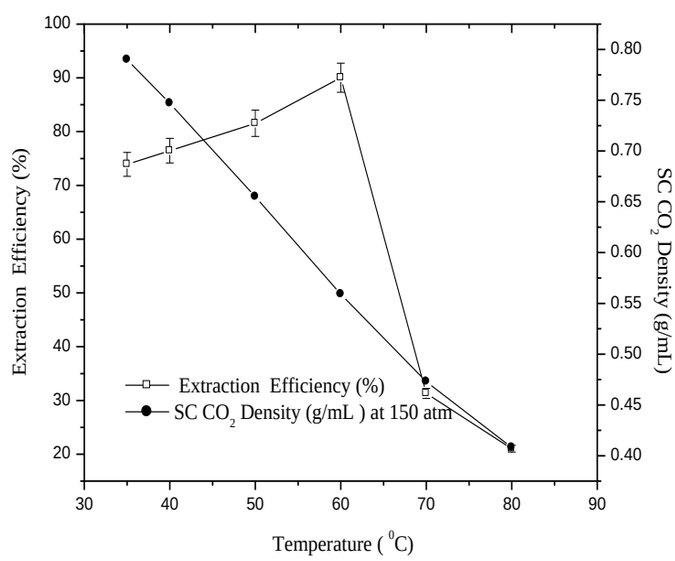

Graph of temperature versus uranium extraction efficiency / SC CO_2 density
(Error bar is ± 3% of the value)

References

1. Irish, E.R., Reas, W.H.: USAEC report TID –7534 (1957).
2. Hanny, J. B., Hogarth, J.: Proceedings of Royal Soc. (London) **29**, 324(1879).
3. Lovelock, J.: Private communication quoted in W. Bertsch, thesis, University of Houston, Texas, (1958).
3. Klesper, E., Corwin, A. H., Turner, D. A.: J. Org. Chem. **27,** 600 (1962).
4. Hawthorne,S.B., Anal.Chem. **62,** 633 (1990)
5. Laintz K.E., Wai C.M., Yonker C.R, Smith R.D.: Anal. Chem, 64 (1992) 2875.
6. Smart, N.G., Carleson, T., Kast, T., Clifford, A.A., Burford, M.D.,Wai,C.M.:Talanta, **44,**137 (1997).
7. Lin, Y.,Brauer, R.D., Laintz, K.E., Wai, C.M.: Anal.Chem., **65,** 2549 (1993).
8. Lin, Y., Smart, N.G., Wai, C.M.: Environ. Sci. Technol, **29,** 2706 (1995).
9. Chrastil J.: J. Phys. Chem. **86**, 3016 (1982).
10. Meguro, Y., Iso, S., Takeishi, H., Yoshida, Z., Anal. Chem. **70**, 1262 (1998).
11. Meguro, Y., Iso, S., Takeishi, H., Yoshida, Z., Anal. Chem. **70**, 774 (1998).
12. Schurhammer, R., Wipff, G., J. Phys. Chem. A **109**, 5208 (2005)

Nobel Prize in Chemistry : 2020

Compilation by
Dr. Dr. Pradeep Kumar

Senior Scientist, Bhabha Atomic Research Centre, Trombay

Chief editor and Vice president ISAS.

The Nobel Prize in Chemistry 2020 was awarded jointly to Emmanuelle Charpentier and Jennifer A. Doudna "for the development of a method for genome editing."

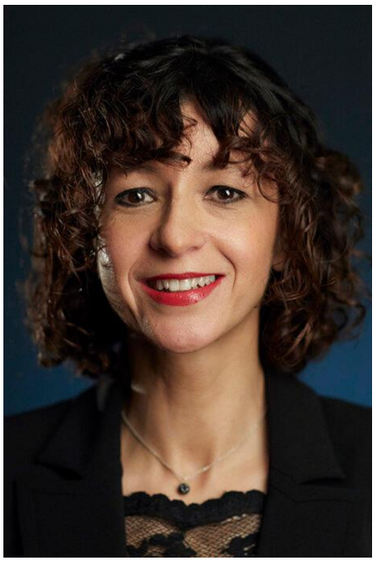

Emmanuelle Charpentier

Max Planck Unit for the Science of Pathogens, Berlin, Germany

Emmanuelle Charpentier , born 1968 in Juvisy-sur-Orge, France.

Ph.D. 1995 from Institut Pasteur, Paris, France. Director of the Max Planck

Unit for the Science of Pathogens, Berlin, Germany

Jennifer A. Doudna

University of California, Berkeley, USA

Jennifer A. Doudna , born 1964 in Washington, D.C, USA. Ph.D. 1989 from

Harvard Medical School, Boston, USA. Professor at the University of California,

Berkeley, USA and Investigator, Howard Hughes Medical Institute.

Genetic scissors: a tool for rewriting the code of life

Emmanuelle Charpentier and Jennifer A. Doudna

have discovered one of gene technology's sharpest tools: the CRISPR/Cas9 genetic scissors. Using these, researchers can change the DNA of animals, plants and microorganisms with extremely high precision. This technology has had a revolutionary impact on the life sciences, is contributing to new cancer therapies and may make the dream of curing inherited diseases come true.

Researchers need to modify genes in cells if they are to find out about life's inner workings. This used to be time-consuming, difficult and sometimes impossible work. Using the CRISPR/Cas9 genetic scissors, it is now possible to change the code of life over the course of a few weeks. "There is enormous power in this genetic tool, which affects us all. It has not only revolutionised basic science, but also resulted in innovative crops and will lead to ground-breaking new medical treatments," says Claes Gustafsson, chair of the Nobel Committee for Chemistry.

As so often in science, the discovery of these genetic scissors was unexpected. During Emmanuelle Charpentier's studies of Streptococcus pyogenes, one of the bacteria that cause the most harm to humanity, she discovered a previously unknown molecule, tracrRNA. Her work showed that tracrRNA is part of bacteria's ancient immune system, CRISPR/Cas, that disarms viruses by cleaving their DNA. Charpentier published her discovery in 2011. The same year, she initiated a collaboration with Jennifer Doudna, an experienced biochemist with vast knowledge of RNA. Together, they succeeded in recreating the bacteria's genetic scissors in a test tube and simplifying the scissors' molecular components so they were easier to use.

In an epoch-making experiment, they then reprogrammed the genetic scissors. In their natural form, the scissors recognise DNA from viruses, but Charpentier and Doudna proved that they could be controlled so that they can cut any DNA molecule at a predetermined site. Where the DNA is cut it is then easy to rewrite the code of life.

Since Charpentier and Doudna discovered the CRISPR/Cas9 genetic scissors in 2012 their use has exploded. This tool has contributed to many important discoveries in basic research, and plant researchers have been able to develop crops that withstand mould, pests and drought. In medicine, clinical trials of new cancer therapies are underway, and the dream of being able to cure inherited diseases is about to come true. These genetic scissors have taken the life sciences into a new epoch and, in many ways, are bringing the greatest benefit to humankind.

Streptococcus' natural immune system against viruses: CRISPR/Cas9

When viruses infect a bacterium, they send their harmful DNA into it. If the bacterium survives the infection, in inserts a piece of the virus DNA in its genome, like a memory of the virus. This DNA is then used to protect the bacterium from new infections.

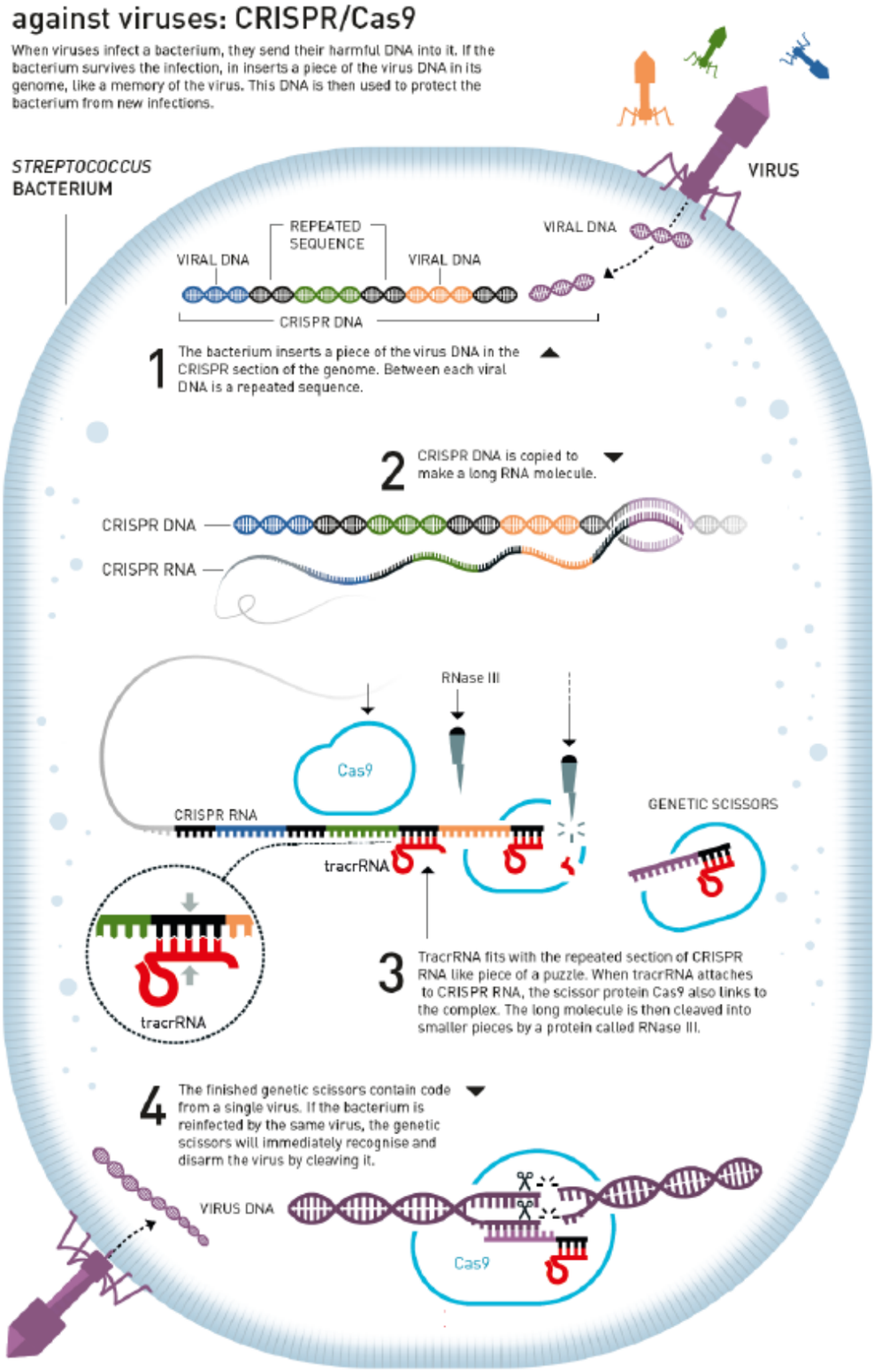

The CRISPR/Cas9 genetic scissors

When researchers are going to edit a genome using the genetic scissors, they artificially construct a guide RNA, which matches the DNA code where the cut is to be made. The scissor protein, Cas9, forms a complex with the guide RNA, which takes the scissors to the place in the genome where the cut will be made.

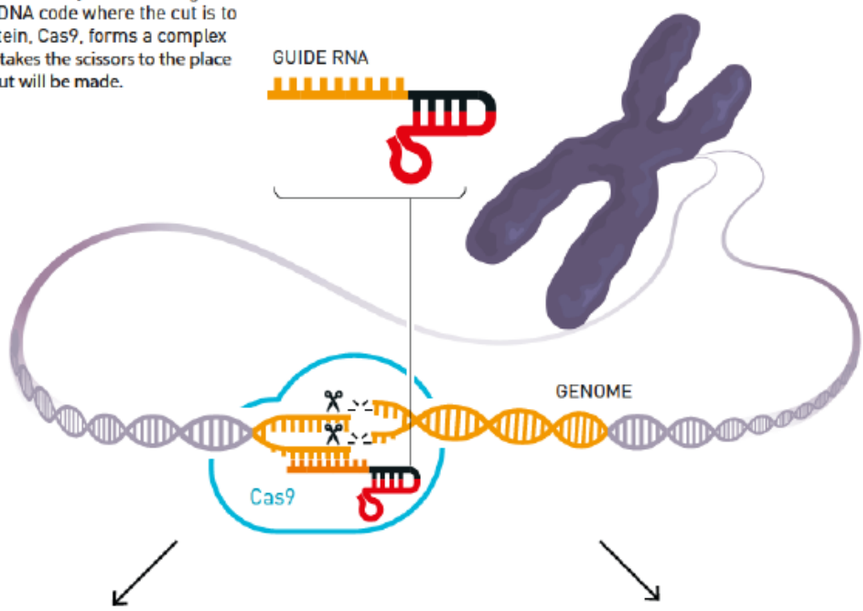

A

Researchers can allow the cell itself to repair the cut in the DNA. In most cases, this leads to the gene's function being turned off.

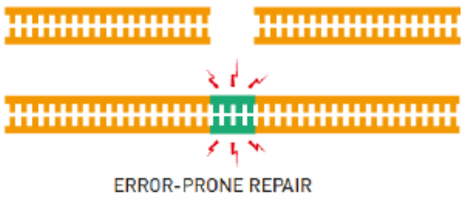

B

If the researchers want to insert, repair or edit a gene, they can specially design a small DNA template for this. The cell will use the template when it repairs the cut in the genome, so the code in the genome is changed.

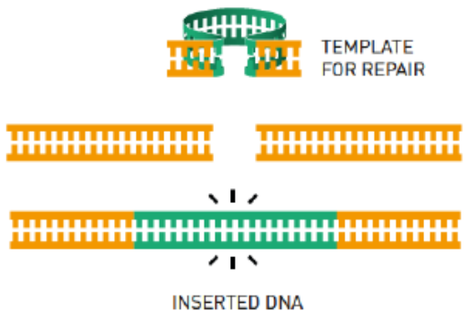

Introduction

In 1953, J.D. Watson and F.H.C. Crick reported the molecular structure of DNA [1]. Ever since, scientists have tried to develop technologies that can manipulate the genetic material of cells and organisms. With the discovery of the RNA-guided CRISPR-Cas9 system, an easy and effective method for genome engineering has now become a reality. The development of this technology has enabled scientists to modify DNA sequences in a wide range of cells and organisms. Genomic manipulations are no longer an experimental bottleneck. Today, CRISPR-Cas9 technology is used widely in basic science, biotechnology and in the development of future therapeutics [2].

The discovery of the CRISPR-Cas system in prokaryotes.

The work that eventually led to the discovery of the powerful CRISPR-Cas9 system for genome editing began with the identification of repeated genome structures present in bacteria and Archaea. In 1987, a report noted an unusual repeated structure in the *Escherichia coli* genome, which contained five highly homologous sequences of 29 base pairs (bp), including a dyad symmetry of 14 bp that were interspersed by variable spacer sequences of 32 bp [3]. Some years later, similar, repeated structures were identified in the genome of the halophilic Archaea *Haloferax mediterranei*, with 14 almost perfectly conserved sequences of 30 bp, repeated at regular distances [4].

Subsequent bioinformatics analyses revealed that these types of repeats were common in prokaryotes and all contained the same peculiar features: a short, partially palindromic element occurring in clusters and separated by unique intervening sequences of constant length, suggesting an ancestral origin and high biological relevance [5]. The term CRISPR was introduced, an abbreviation for clustered regularly interspaced short palindromic repeats [6].

An important step towards understanding the function of CRISPR came with the identification of CRISPR-associated (*cas*) genes, a group of genes only present in CRISPR-containing prokaryotes and always located adjacent to CRISPRs. The identified *cas* genes encoded proteins with helicase and nuclease motifs suggesting a role in DNA metabolism or gene expression [6]. The association with CRISPR was used as a defining characteristic and over the coming years a number of Cas protein subfamilies were described [7, 8].

The functional importance of the CRISPR loci remained elusive until 2005, when researchers noted that the unique CRISPR sequences were derived from transmissible genetic elements, such as bacteriophages and plasmids [9-11]. Prokaryotes carrying these specific sequences appeared protected from infection, since plasmids or viruses containing a sequence matching a spacer (named protospacers) were usually absent in the prokaryote carrying the spacer [9, 11].

These correlative findings suggested a function for CRISPRs in prokaryotic defence against invading foreign DNA and the spacer sequences were described as a ‘memory of past “genetic aggressions”’ [10]. It had already been shown that CRISPRs were transcribed into long RNA

molecules (pre-crRNA), which were subsequently processed by cleavage within the repeat sequences to yield small CRISPR-RNAs (crRNAs) [4, 12]. Taken together these observations indicated that crRNA could play a role in targeting viral nucleic acids, perhaps in a manner similar to RNAi in eukaryotic cells. It was also hypothesized that the Cas proteins was involved in this process [9].

Later research has indeed demonstrated that crRNA binds to one or more Cas proteins to form an effector complex that targets invading nucleic acids. Extensive efforts during the past 25 years have identified a number of different CRISPR-Cas systems, which are now divided into two major classes

[13]. In the Class 1 systems, specialised Cas proteins assemble into a large CRISPR-associated complex for antiviral defence (Cascade). The Class 2 systems are simpler and contain a single multidomain crRNA-binding protein (e.g. Cas9) that contains all the activities necessary for interference.

CRISPR-Cas functions as an adaptable defence system

The hypothesis that CRISPR-Cas systems could confer resistance to invading foreign DNA was verified in 2007 [14]. In an elegant set of experiments, scientists studied a Class 2 system in a strain of *Streptococcus thermophilus*, which they infected with virulent bacteriophages. Next, bacteria resistant to infection were isolated and their CRISPR loci analysed. The experiment revealed that resistant bacteria had acquired new spacer sequences, which matched sequences within the infecting phage used to select resistance. Deletion of the spacer region led to loss of resistance, and the phages that were able to grow on resistant bacteria had accumulated mutations in the protospacer sequence in the phage genome. Furthermore, inactivation of one of the *cas* genes (*cas5*) resulted in loss of phage resistance. The experiments thus demonstrated a role for *cas* gene products in CRISPR-Cas–mediated immunity and that the specificity of the system was dependent on the spacer sequences [14].

Further insights into the function of CRISPR-Cas came from investigations of *E. coli*, which contains a Class 1 CRISPR-Cas system encoding no less than eight different Cas proteins. Five of these gene products could be purified as a multiprotein complex termed Cascade (CRISPR-associated complex for antiviral defence). Cascade was shown to function in pre-crRNA processing, cleaving the long transcripts in the repeated regions and thereby producing shorter crRNA molecules containing the virus-derived sequence [15]. After cleavage, the mature crRNA molecules were retained by Cascade, and, assisted by a *cas*-encoded helicase, Cas3, they served as guide molecules that enabled Cascade to interfere with phage proliferation. The results thus suggested two different steps in CRISPR function: first, CRISPR expression and crRNA maturation, and second, an interference step that required the Cas3 protein. The results also provided evidence suggesting that the *E. coli* CRISPR-Cas system targets phage DNA and not RNA, inasmuch as crRNA with complementarity to either of the two DNA strands could interfere with phage proliferation [15].

Conclusive evidence for DNA being the target of CRISPR-Cas interference came from elegant experiments using a strain of *Staphylococci epidermidis* that contained a CRISPR array with a spacer sequence homologous to a gene present in a conjugative plasmid [16]. Transfer of the plasmid into the strain occurred only if the spacer sequence was mutated or deleted. A self-splicing intron was inserted into the target sequence on the plasmid. In this way, the CRISPR spacer would be complementary not to the DNA, as it is disrupted by an intron, but to the RNA, which would be spliced, reconstituting the sensitive target. Indeed, insertion of the self-splicing intron was sufficient to overcome CRISPR-Cas inhibition of plasmid transfer, strongly implicating

DNA as the primary target [16]. This conclusion was further supported from studies of *S. thermophilus*, in which the CRISPR-Cas system was shown to cleave both bacteriophage and plasmid DNA *in vivo* [17].

Protospacer adjacent motifs distinguish CRISPR from invading DNA.

If spacers lead to cleavage of DNA with matching sequences, how do they avoid cleaving their own CRISPR spacers? The answer to this question came from studies of sequences around protospacers, i.e. the sequences in the phage genomes that had given rise to spacers. Short sequence motifs were noted just a couple of nucleotides away from protospacer sequences [11, 18]. These motifs were later labelled protospacer adjacent motifs or PAMs [19].

The functional importance of PAMs became clear from work studying the phage response to CRISPR-encoded resistance in *S. thermophilus*. In these studies, phages that had overcome bacterial resistance were isolated and analysed. These studies revealed that a number of those resistant to CRISPR immunity had acquired mutations in the PAMs, implicating these short sequences as important for targeting [20]. Later studies have demonstrated that the PAM sequences are required both for target interference and for uptake of new spacer sequences into CRISPRs [21, 22].

Discovery of the CRISPR-Cas9 system

By 2011, it was clear that CRISPR-Cas systems were widespread in prokaryotes and functioned as adaptive immune systems to combat invading bacteriophages and plasmids (Figure 1). Studies had also established that the Cas proteins functioned at three different levels: (i) integration of new spacer DNA sequences into CRISPR loci, (ii) biogenesis of crRNAs, and (3) silencing of the invading nucleic acid [23, 24].

The identification of CRISPR-Cas9 as a tool for genomic editing came from studies of the Class-2, Type-II CRISPR-Cas system in *S. thermophilus* and the related human pathogen *Streptococcus pyogenes*. This system contains four *cas* genes, three of which (*cas1*, *cas2*, *csn2*) are involved in spacer acquisition, whereas the fourth, *cas9* (formerly named *cas5* and *csn1*), is needed for interference [14]. In support of this notion, inactivation of the *cas9* gene prevented cleavage of target DNA [17]. To further define the elements required for immunity, the *S. thermophilus* CRISPR-Cas system was introduced into *E. coli*, where it provided heterologous protection against infection with phages and plasmids [25]. Using this experimental model, parts of the system were inactivated to define the components required for protection. The work clearly demonstrated that the Cas9 protein alone was sufficient for the CRISPR-encoded interference step, and that two nuclease domains present in the protein, HNH and RuvC, were both required for this effect [25].

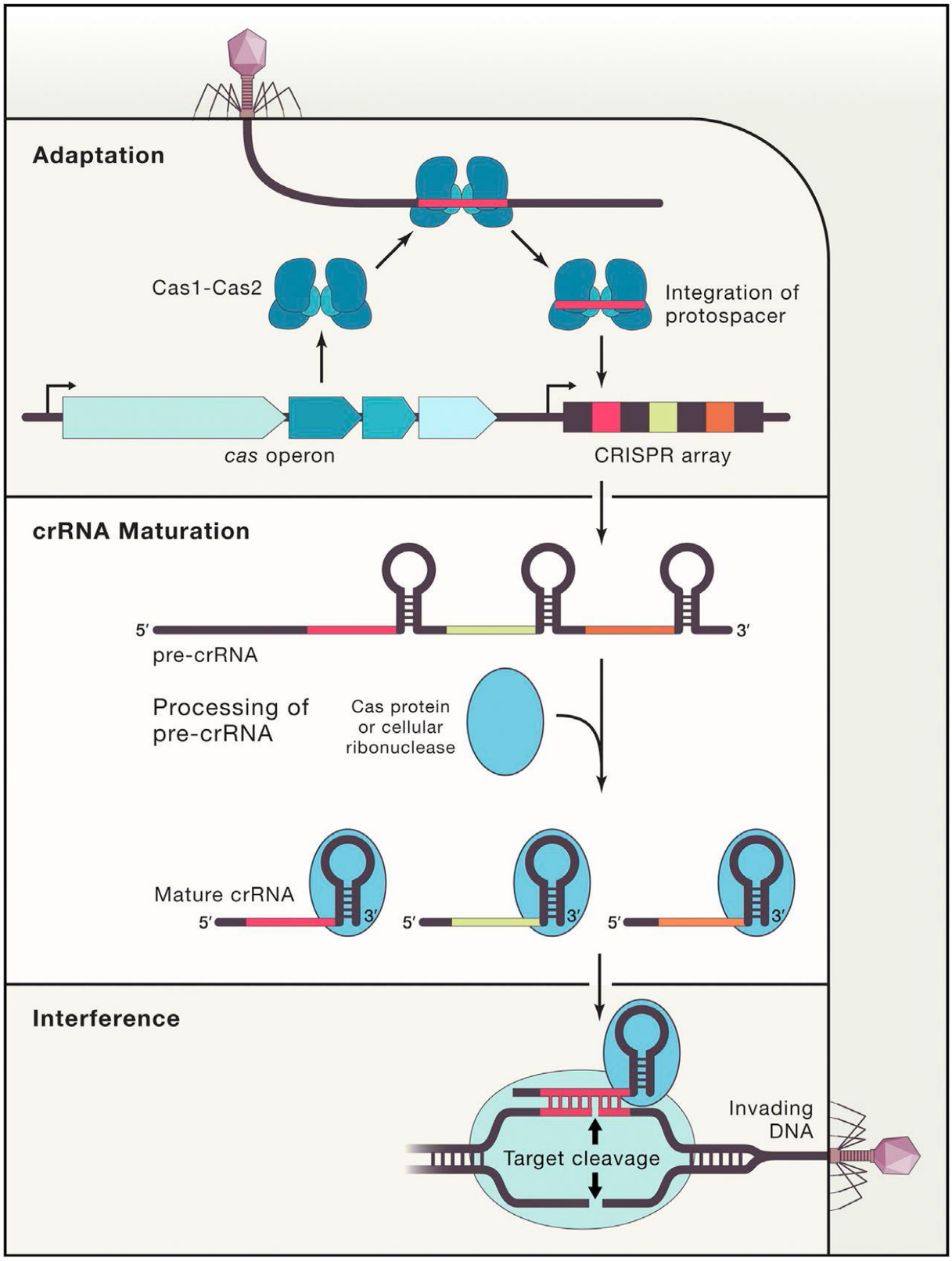

Figure 1. A general scheme for the function of the CRISPR-Cas adaptive immune system as presented in [26]. Three stages are identified. Adaptation: Short fragments of double-stranded DNA from a virus or plasmid are incorporated into the CRISPR array on host DNA. crRNA Maturation: Pre-crRNA are produced by transcription and then further processed into smaller crRNAs, each containing a single spacer and a partial repeat. Interference: Cleavage is initiated when crRNA recognize and specifically base-pair with a region on incoming plasmid or virus DNA. Interference can be separated both mechanistically and temporally from CRISPR acquisition and expression.

Discovery of tracrRNA and its role in crRNA maturation

In 2011, **Emmanuelle Charpentier** and colleagues reported on the mechanisms of crRNA maturation in *S. pyogenes* [27]. Using differential RNA sequencing to characterize small, non-coding RNA molecules, they identified an active CRISPR locus, based on expression of pre-crRNA and mature crRNA molecules. Unexpectedly, the sequencing efforts also identified an abundant RNA species

transcribed from a region 210 bp upstream of the CRISPR locus, on the opposite strand of the CRISPR array (Figure 2a).

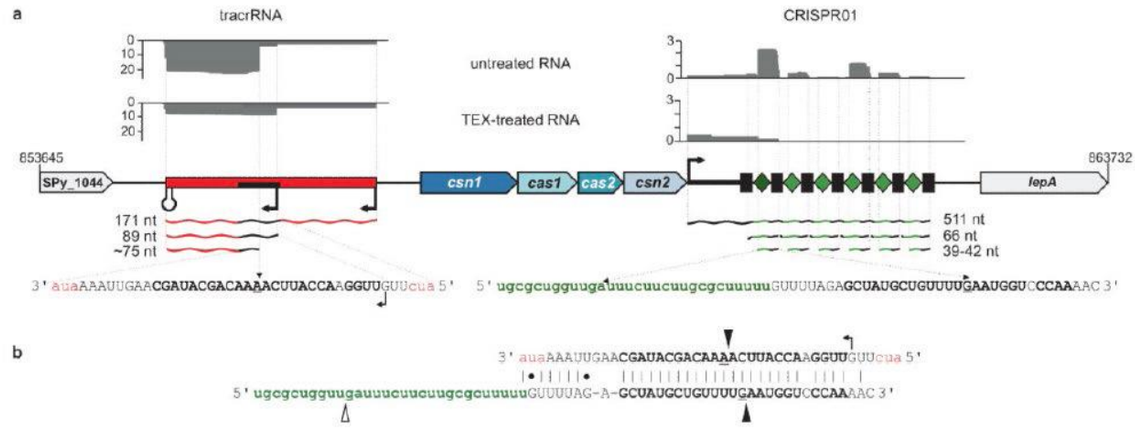

Figure 2. Identification of tracrRNA in *S. pyogenes* as reported in [27]. **a.** Differential RNA sequencing (dRNA-seq) reveals expression of tracrRNA and crRNAs. Sequence reads of cDNA libraries of RNA are shown on top. Below is the genomic organisation of tracrRNA and CRISPR01/Cas loci. Red bar: tracrRNA is encoded on the minus strand and detected as 171-, 89- and ~75-nt tracrRNA species. Black rectangle inside the red bar: 36-nt sequence stretch complementary to CRISPR01 repeat. The pre-crRNA is encoded on the plus strand. Black rectangles: CRISPR01 repeats; green diamonds: CRISPR01 spacers; 511, 66 and 39-42 nt: pre-crRNA and processed crRNAs. **b.** Base-pairing of tracrRNA with a CRISPR01 repeat is represented. Cleavages observed by dRNA-seq and leading to the formation of short overhangs at the 3′ ends of the processed RNAs are indicated by two black triangles.

The transcript was denoted *trans*-encoded small RNA (tracrRNA) and contained a stretch of 25 nucleotides (nt) with almost perfect complementarity (1-nt mismatch) to the repeat regions of the CRISPR locus, thus predicting base pairing with pre-crRNA [27]. The RNA duplex region that would form included processing sites for both pre-crRNA and tracrRNA, which immediately suggested that the two RNAs could be co-processed upon pairing (Figure 2b).

In support of the proposed idea, deletion of the tracrRNA locus prevented pre-crRNA processing and vice versa. Charpentier and colleagues also noted that a co-processed duplex involving tracrRNA and pre-crRNA would have short 3′ overhangs, similar to those produced by the endoribonuclease RNase III, and they went on to demonstrate that this enzyme could process a heteroduplex formed between tracrRNA and pre-crRNA in vitro and was required for tracrRNA and pre-crRNA processing in vivo. Finally, the researchers found that processing also involved the Cas9 protein, since deletion of the cas9 gene in bacteria impaired both tracrRNA and pre-crRNA processing. Based on their findings, Charpentier and coworkers suggested that the Cas9 protein acts as a molecular anchor that facilitates base pairing between tracrRNA and pre-crRNA,

which in turn allows recognition and cleavage by the host RNase III protein [27].

Previous reports had revealed the importance of Cas9 for interference. Charpentier and Jennifer A. Doudna initiated a collaboration to investigate if crRNA could be used to direct the sequence specificity of the nuclease. In contrast to what had been hypothesised in Charpentier's report a year earlier, addition of crRNA to purified Cas9 could not stimulate Cas9-catalysed target DNA cleavage [27, 28].

At this point, the two scientists made a crucial discovery. Addition of tracrRNA to the in vitro reaction triggered Cas9 to cleave the target DNA molecule. The tracrRNA thus had two critical functions:

triggering pre-crRNA processing by the enzyme RNase III and subsequently activating crRNA-guided DNA cleavage by Cas9.

In a series of in vitro biochemistry experiments, the researchers investigated the biochemical mechanisms of the reaction [28]. The two nuclease domains in Cas9, HNH and RuvC, were each shown to cleave one strand of target DNA. Cleavage occurred 3 bp upstream of the PAM sequence, which in S. pyogenes has the sequence 5′-NGG-3′, with N corresponding to any of the four DNA bases. Furthermore, as predicted from previous reports, target recognition and cleavage were inhibited by mutations in the PAM sequence [20].

A peculiar aspect of PAM sequence dependence was that cleavage of double-stranded DNA was sensitive to mutations in both the complementary and non-complementary strand whereas cleavage of single-stranded DNA targets was unaffected by mutations in the PAM motif. These observations led the authors to conclude that PAM motifs may be required to allow duplex unwinding [28].

Similar findings were also published in another report using the related CRISPR-Cas system in Streptococcus thermophilus. As in Charpentier and Doudna's work, this report also demonstrated that Cas9 cleaves within the protospacer, that cleavage specificity is directed by the crRNA sequence, and that the two nuclease domains within Cas9, each cleave one strand. However, the researchers did not notice the crucial importance of tracrRNA for sequence-specific cleavage of target DNA [29].

In their study, Charpentier, Doudna and colleagues also worked to delineate the regions of tracrRNA and crRNA that are absolutely required for Cas9-catalysed cleavage of target DNA. This led to the identification of an activating domain in tracrRNA and the realisation that a "seed region" of ∼10 nt in the PAM-proximal region of the target strand was especially important for target recognition.

Based on their in vitro biochemical analysis, the authors hypothesized that the structural features in the two RNA molecules required for Cas9-catalysed DNA cleavage could be captured in a single RNA molecule. In a crucial experiment, they demonstrated that this was indeed possible: the RNA components (crRNA and tracrRNA) of the Cas9 complex could be fused together to form an active, chimeric single-guide RNA molecule (sgRNA).

Furthermore, Charpentier and Doudna demonstrated that the sequence of the chimeric sgRNA could be changed so that CRISPR-Cas9 would target DNA sequences of interest, with the only constraint being the presence of a PAM sequence adjacent to the targeted DNA. They had

thus created a simple two-component endonuclease, containing sgRNA and Cas9, that could be programmed to cleave DNA sequences at will.

The importance of this finding was not lost on them. In the abstract of the paper reporting their findings, the authors wrote: "Our study reveals a family of endonucleases that use dual-RNAs for site-specific DNA cleavage and highlights the potential to exploit the system for RNA programmable genome editing" [28].

A molecular understanding of the CRISPR mechanism

Today, there is a detailed structural understanding of how the Cas9-gRNA complex recognizes its target and mediates cleavage. This information has been important for efforts to engineer new versions of the system, with altered PAM specificity and reduced off-target activities [30].

The structure of Cas9 in free form revealed two distinct lobes, the recognition (REC) lobe and the nuclease (NUC) lobe, with the latter containing the HNH and RuvC nuclease domains. When Cas9 binds to sgRNA, it undergoes a structural rearrangement, with the REC lobe moving towards the HNH domain (Figure 3).

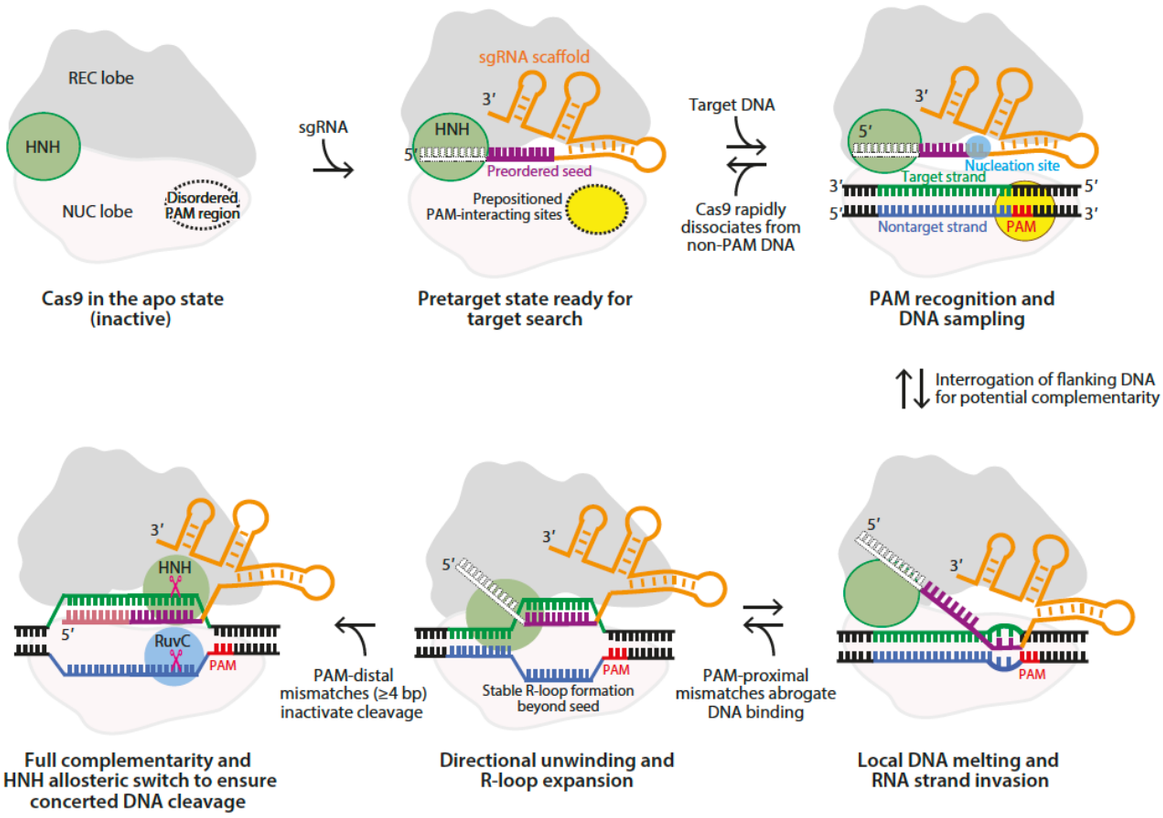

Figure 3. A schematic representation of the mechanism by which CRISPR-Cas9 recognizes and targets DNA for cleavage as presented in [30]. Binding of sgRNA leads to a large conformational change in Cas9. In this activated conformation, the PAM-interacting cleft (dotted circle), becomes pre-structured for PAM sampling, and the seed sequence of sgRNA is positioned to interrogate adjacent DNA for complementarity to sgRNA. The process starts with PAM recognition, which in the next step leads to local DNA melting and RNA strand invasion. There is a step-wise elongation of the R-loop formation and a conformational change in the HNH domain to ensure concerted DNA cleavage. Abbreviations: bp, base pair; NUC, nuclease lobe; PAM, protospacer adjacent motif; REC, recognition lobe; sgRNA, single-guide RNA.

For target recognition, the 20-nt spacer sequence must form complementary base pairs with the protospacer sequence. In the structure of Cas9 in complex with sgRNA, the 10-nt seed sequence in the spacer adopts an A-form conformation and is positioned to engage with the target sequence in DNA [31, 32]. The seed sequence is located in the 3′ end of the 20-nt spacer sequence and is essential for target recognition [25, 28, 33]. In genome editing, similarities between the seed sequence and genome sequences can cause off-target effects, even if there are many mismatches elsewhere in the spacer region of sgRNA [34].

As noted, a PAM sequence must also be present next to the target site, and mutations in this motif prevent Cas9-dependent cleavage at the target sequence. The Cas9 protein first searches for the PAM sequence, and once found, probes the flanking DNA for complementarity to the sgRNA. The GG dinucleotides in PAM are recognized by base-specific hydrogen-bonding interactions with two arginine residues in a PAM interacting site, which is disordered in the apo-form of Cas9, but becomes ordered after sgRNA binding. The interactions between PAM and Cas9/sgRNA lead to destabilization of the adjacent double-stranded DNA, which in turn facilitates for sgRNA to invade the double-stranded DNA. The destabilization is in part explained by a kink in the target DNA strand, which is

caused by Cas9 interactions with the phosphate group immediately upstream of the PAM in the same strand [22].

Once a stable RNA–DNA duplex, an R-loop, has been formed, Cas9 is activated for DNA cleavage. Each of the two nuclease domains cleaves one strand of the target double-stranded DNA at a specific site 3 bp from the 5′-NGG-3′ PAM sequence, and in most cases, the ends that are formed are blunt. By inactivating one of the two domains, a nickase can be formed, i.e. an enzyme that cleaves only one strand of a DNA duplex [28, 29]. Nickases are very useful for practical applications of CRISPR-Cas systems, since they can be programmed to target opposite strands and thus make staggered cuts within the target DNA. In this way, a Cas9 nickase mutant, combined with a pair of sgRNA molecules, can introduce targeted double-strand breaks with very high sequence specificity [35].

The application of the CRISPR-Cas9 technology in higher cells

Genome editing relies on the existence of natural pathways for DNA repair and recombination. Double-stranded breaks typically lead to either non-homologous end joining (NHEJ) repair or homology-directed repair (HDR). In the case of NHEJ, the ends are directly ligated back together and the process usually results in a small insertion or deletion of DNA at the break, frequently causing frame shifts in coding sequences and loss of protein expression. The HDR pathway instead uses a homologous DNA sequence as a template to repair the break. By introducing modified genetic sequences as templates for the HDR, it is thus possible to introduce defined genomic changes such as base substitutions or insertions.

DNA can be introduced into mice embryonic stem cells and recombine there with the matching sequence within the host genome to produce gene-modified animals. This method is powerful but labour-intensive, since recombination events are rare and require a selectable marker, such as an antibiotic resistance gene, to be identified. Recombination efficiency is enhanced if a double-stranded break is introduced at the site of the desired recombination event, which led to a search for endonucleases that can be programmed to cleave DNA at locations of interest.

An important earlier step in the engineering of sequence-specific nucleases came with the development of zinc finger nucleases (ZFNs) and transcription activator–like effector nuclea

(TALENs). When linked to a nuclease domain, zinc finger proteins can function as site-specific nucleases that can cleave genomic DNA in a sequence-specific manner and stimulate site-specific recombination [36, 37]. TALENs provide yet another DNA-binding modality that recognizes DNA in a modular fashion and that can be fused to nuclease domain [38]. Both ZFNs and TALENs are powerful tools for genome editing. However, their widespread use has been limited by the inherent difficulties of protein design, synthesis and validation.

In their work, **Charpentier** and **Doudna** defined a simple two-component system that could rapidly be programmed for sequence-specific cleavage of target DNA and thereby sparked a revolution in genome editing. The first experimental demonstration that CRISPR-Cas9 could indeed be harnessed for genome editing in human and mouse cells came in early 2013 [39, 40]. These influential studies demonstrated that Cas9 nucleases could be directed by crRNA of a defined sequence to induce precise cleavage at endogenous genomic loci in mouse and human cells. For the reaction to occur, tracrRNA, crRNA, and Cas9 were all required, whereas RNase III was replaced by endogenous enzyme activities. Just as observed by **Charpentier** and **Doudna** *in vitro*, the system could be further simplified *in vivo*, and a chimeric sgRNA molecule together with Cas9 was sufficient to cleave target DNA. The system has also been used to introduce genome modification in a number of other eukaryotic systems [41],

including *Saccharomyces cerevisiae*, *Drosophila melanogaster*, *Caenorhabditis elegans*, *Danio rerio* and *Arabidopsis thaliana* [42-46], demonstrating its broad applicability.

In ongoing work, scientists are trying to expand the usefulness of the CRISPR-Cas system for genome editing. In addition to Cas9 from *S. pyogenes*, a number of other Cas homologues are used today for genome editing and related purposes. Naturally occurring CRISPR systems have other PAM requirements, and in addition, new Cas9 variants are continually engineered to have altered PAM compatibilities. CRISPR-Cas systems can also be used to target RNA. Studies of *Pyrococcus furiosus* demonstrated that in this species, the system encodes for a crRNA-guided Cas complex, which targets foreign mRNA [47].

Efforts are also under way to develop evermore precise CRISPR-Cas–based genome editing strategies [48]. These efforts include strategies for base editing at specific sites in eukaryotic genomes (Figure 4). As an example, a cytidine deaminase enzyme has been fused to a mutant form of Cas9 that cleaves only one strand – a nickase. When programmed with sgRNA for the desired sequence, this system can be targeted to a specific genomic location, induce a nick in the DNA there, and mediate the direct conversion of cytidine to uridine, which after replication results in a cytosine-to-thymine conversion [49].

Another elegant example is a method called prime editing, in which a Cas9 nickase is fused to a reverse transcriptase enzyme [50]. In this approach, the sgRNA contains an additional piece of RNA, creating a "prime editing guide RNA" that both specifies the target site and encodes the desired edit. Once produced by the reverse transcriptase, the DNA synthesized can be installed at the nick, replacing one of the original DNA sequences.

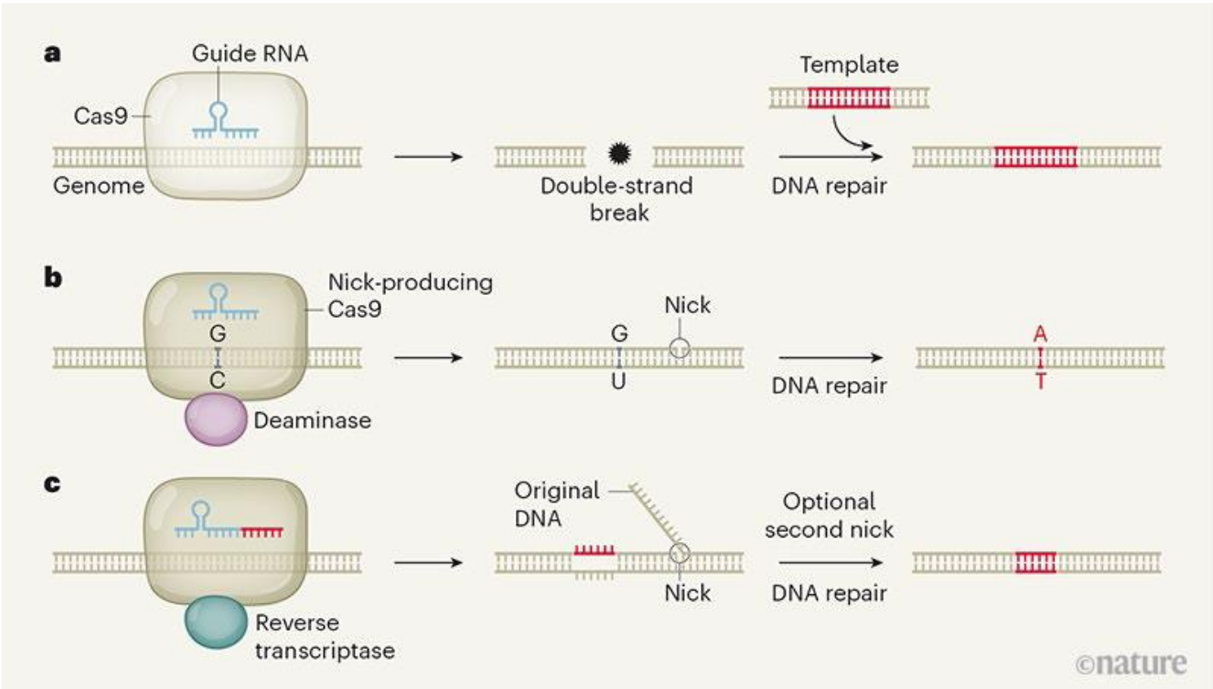

Figure 4. Genome editing with Cas9 as presented in [48]. **a.** The Cas9 enzyme is directed to target DNA by a guide RNA and produces a double-stranded break. A piece of DNA can be used as a template for homology-directed repair (HDR). **b.** Cas9 can be fused to a deaminase enzyme. The mutant Cas9 produces a nick, which stimulates deaminase activity. The deaminase converts a cytidine base (C) to uracil (U). DNA repair then repairs the nick and converts a guanine–uracil (G–U) intermediate to an adenine–thymine (A–T) base pair. **c.** Prime editing. A nick-producing Cas9 and a reverse transcriptase enzyme produce nicked DNA, into which sequences corresponding to the guide RNA have been incorporated. The original DNA sequence is cut off, and DNA repair then fixes the nicked strand to produce a fully edited duplex.

Concluding remarks

In 2012, Charpentier and Doudna reported “that the Cas9 endonuclease can be programmed with guide RNA engineered as a single transcript to cleave any double-stranded DNA sequence” [28]. Their discovery has led to widespread applications of the CRISPR-Cas9 system as a powerful and versatile tool in genome editing.

By introducing a vector encoding the Cas9 nuclease and an engineered sgRNA, scientists are now able to make precise single-base-pair changes or larger insertions. Coupled with the availability of genome sequences for a growing number of organisms, the technology allows researchers to explore these genomes to find out what genes do, move mutations that are identified as associated with disease into systems where they can be studied and tested for treatment, or where they can be tested in combinations with other mutations. The technology has enabled efficient targeted modification of crops and is currently being developed to treat and cure genetic diseases, for instance by modifying hematopoietic stem cells to treat sickle cell disease and β-thalassemia.

Finally, it should be emphasised that the power of the CRISPR-Cas9 technology also raises serious ethical and societal issues. It is of utmost importance that the technology is carefully regulated and used in responsible manner. To this end, the World Health Organization has recently established a global multi-disciplinary expert panel to examine the scientific, ethical, social and legal challenges associated with human genome editing, with the aim to develop a global governance framework for human genome editing.

Design and development of Optics for High Energy, High Power Nd:glass Lasers

A.S. JOSHI
Former Head, Advanced Lasers and Optics Division
RAJA RAMANNA CENTRE FOR ADVANCED TECHNOLOGY
jonandan31@gmail.com

Historical Developments of HEHP Nd:glass Lasers

1963	Lebedev Physics Institute (USSR)	Proposal to use lasers for controlled fusion
1968	Lebedev Physics Institute (USSR)	Registration of thermonuclear neutrons in laser-prod
1970	CEA Lemeil (France)	Definite neutron yield observed
1972	Livermore Natl. Lab. (USA) Los Alamos Natl. Lab. (USA)	Starting date for the financing for a national ICF program in the USA
	ILE (Japan)	ICF program in Japan
1974	Lebedev Physics Institute (USSR) (FIAN)	Concept of low-entropy compression of shell targets
	Institute of Applied Mathematics	
1975	ILE (Japan)	Indirect drive Cannonball target concept
1977	Livermore Natl. Lab. (USA)	Launching of 10-kJ Nd laser "Shiva"
1978	Los Alamos Natl. Lab. (USA)	Launching of 10-kJ CO_2 laser "Helios"
	ILE (Japan)	Launching of 2-kJ Nd laser GEKKO IV
1979	Livermore Natl. Lab. (USA)	Density of compressed fuel reached 20 g/cm^3
1983	Livermore Natl. Lab. (USA)	Launching of a 20-kJ "Novette" Nd-laser
1983	ILE (Japan)	Launching of 30-kJ Nd laser "GEKKO XII"
1985	ILE (Japan)	Neutron yield 10^{13} LHART target
1985–1989	Livermore Natl. Lab. (USA)	Launching of 130-kJ Nd laser "Nova" (fuel density, neutron yield, 3×10^{13})
1987–1991	ILE (Japan)	~1000 g/cm^3 matter density reached with GEKKO XII
1994	Livermore Natl. Lab. (USA)	Approval of DOE NIF and declassification

Basic Concepts of Inertial Confinement Fusion

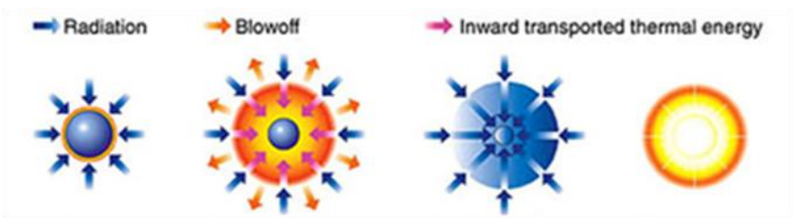

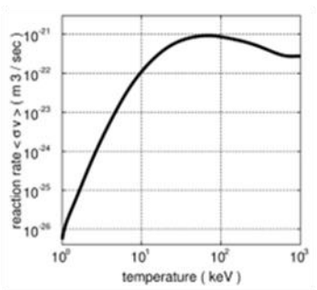

$D+T \rightarrow {}^4He\ (3.5\ MeV) + n(14.1MeV)$

$D+D \rightarrow {}^3He\ (0.82MeV) + n(2.45MeV)$

$D+D \rightarrow T\ (1.01MeV) + p(3.02MeV)$

$D+{}^3He \rightarrow {}^4He\ (3.6MeV) + p(14.7MeV)$

Lawson Criterion for ICF

Parameter	MCF	ICF
Electron density cm^{-3}	10^{14}	10^{25}
Confinement time s	10	10^{-10}
Lawson criterion	10^{15}	10^{15}

Absorption of laser vs. Intensity

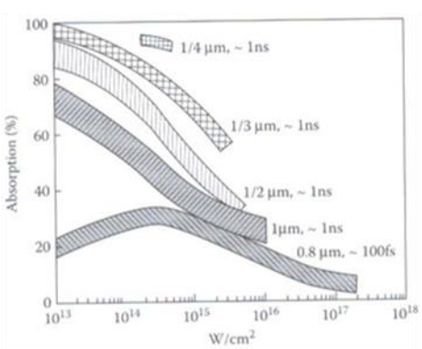

Major HEHP Nd:glass Lasers in the world

Laser Facility	Location	Laser Energy‡	Laser Power ‡	Purpose	Status (approximate year of first operation)
LMJ	France	2.0 MJ	0.6 PW	Defence (10-20% to academic community)	Development (2011)
LIL	France	70 kJ + 4 kJ	0.02 PW + 7PW	Defence + academic user facility	Development (2006 / 2009 PW)
LULI-2000	France	2 kJ	1 PW	Academic user facility	Operational
NIF	USA	1.8 MJ	0.6 PW	Defence (15% to national academic community)	Development (2009)
OMEGA-EP	USA	30 kJ + 5kJ	0.05PW + 2PW	Defence + academic (national programme)	Development (2007 for PW laser) - Operational (implosion laser)
Z-Beamlet	USA	4 kJ	2 PW	Defence + academic (national programme)	Development (2007)
VULCAN	UK	1 kJ + 0.5 kJ	0.001 PW + 1 PW	Academic user facility	Operational
ORION	UK	5 kJ + 1 kJ	0.005 PW + 2 PW	Defence (15% to academic community)	Development (2010)
GEKKO FIREX-I	Japan	10 kJ + 10 kJ	0.01 PW + 1 PW	Academic (national programme)	Development (2007)
FIREX-II	Japan	50 kJ + 50 kJ	0.01 PW + 5 PW	Academic (national programme)	Proposed
PHELIX	Germany	1 kJ	1 PW	Academic	Development (2008)
PALS	Czech	1 kJ	0.003 PW	Academic user facility	Operational
HiPER	Europe	200 kJ + 70 kJ	~10 PW (100 PW option)	Academic user facility	Proposed

Status of development of HEHP Lasers in the world

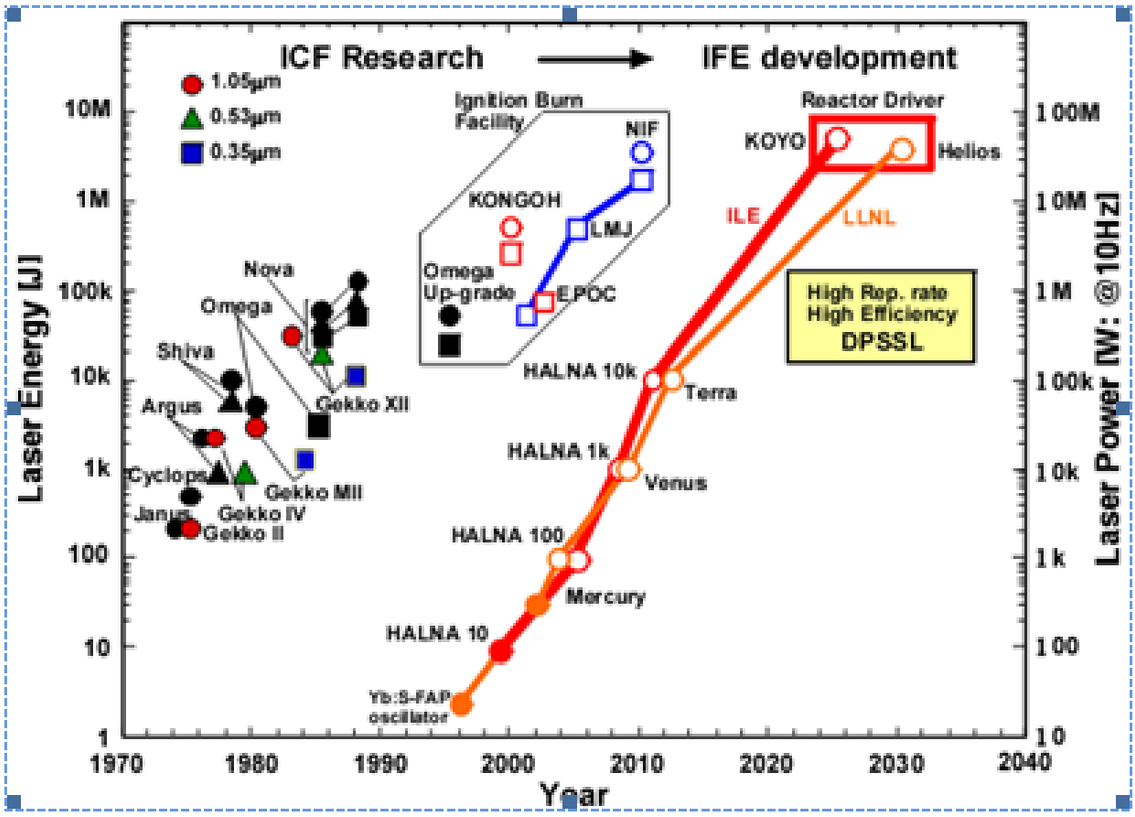

Third Generation HEHP Nd: phosphate glass Laser: NIF

NIF- Largest HEHP Laser

In the world

Main Use: "Nuclear Stock-pile Stewardship"

Energy-1.8 Mega Joules in III Harmonic

192 arms

Largest Nd:Glass slab size 0.5mX1mX.04m

One shot in~8 hours

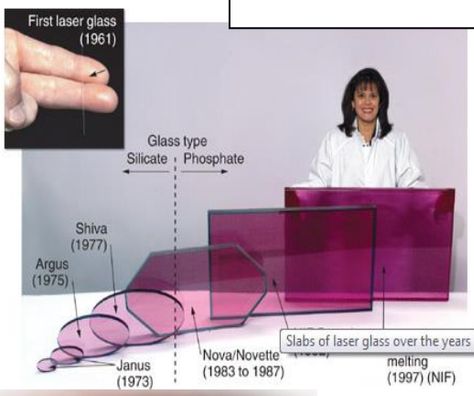

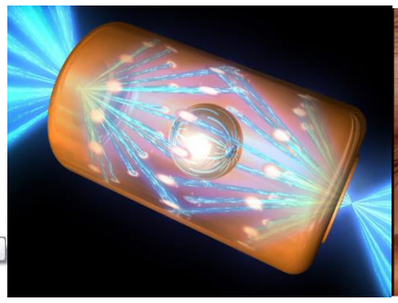

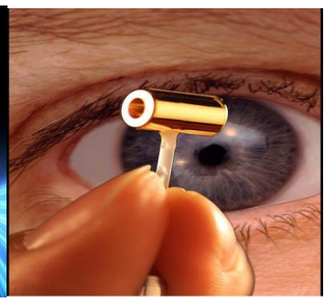

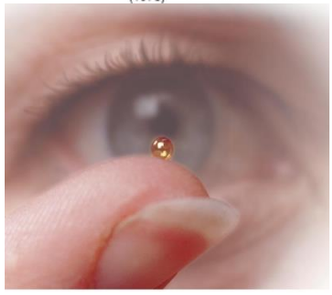

Over view of Four Pass Far Field Disc amplifier (ORION)

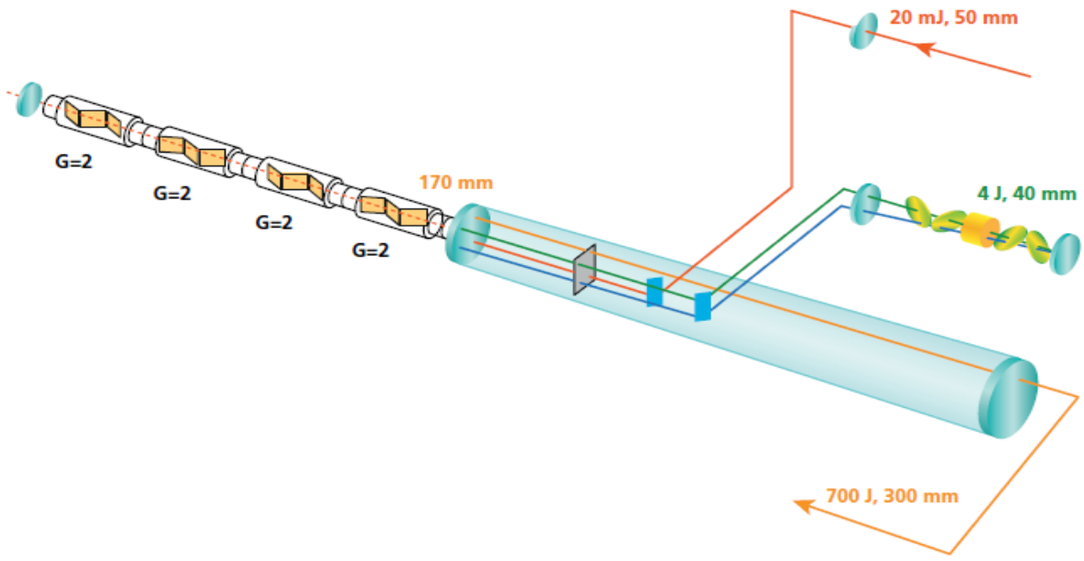

Overview of Transport Spatial Filter and the disk amplifiers.

2 – Arm Nd:glass laser chain(RRCAT)

Two arm HEHP Nd:glass Laser: Overview

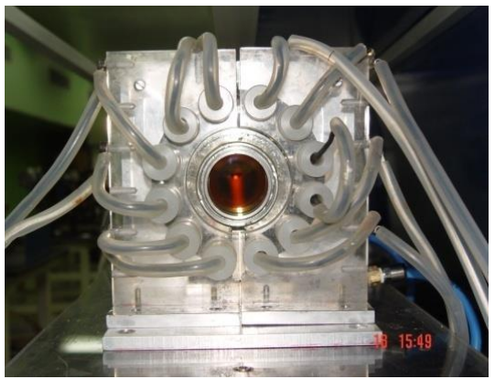

- **Diode pumped SBS based Nd:glass master oscillator (0.5-1.5 ns), KLM Ti: Saphire Laser**
- **Nd:glass laser amplifiers**
  - **12 rod amplifiers (10 mm- 80 mm)**
  - **6 disc amplifiers (100 mm -140 mm)**
- **3 Faraday Isolators (65 mm) each with Isolation of 180 : 1**
- **10 spatial filters - image relay systems**
- **204 Flash lamps (arc length 130 -900 mm) with total electrical pump energy of ~1 MJ**

Spatial filtering and Self focusing of Laser

Inst. Change in ρ(e) leading to change in ref. index.

$n = n_0 + n_2 I(x)$

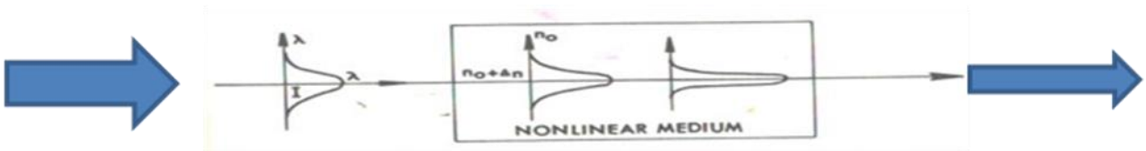

For positive n_2 the refractive index is higher at higher intensities

Threshold for self focusing:

- **Power Threshold for self focusing: ~ 10 MW**
- **Convergence due to self focusing balances divergence due to diffraction**

Operations of the Laser : @ 100GW-100 TW, Hence critical

to control self focusing?

> Choose materials with low n_2 (Phosphate glass Preferred over silicate)

> Sequential relaying and spatial filtering of the laser

Small scale self focusing of High Power Lasers

Beam Diameter 100 mm (simulations)

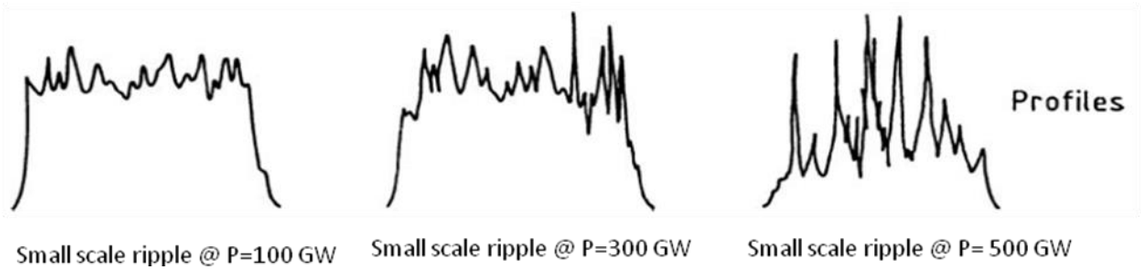

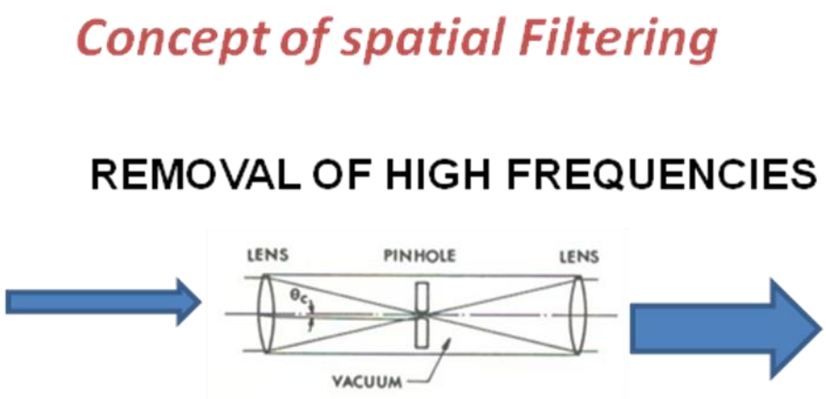

Development of Nd doped phosphate laser glass rods/discs in India

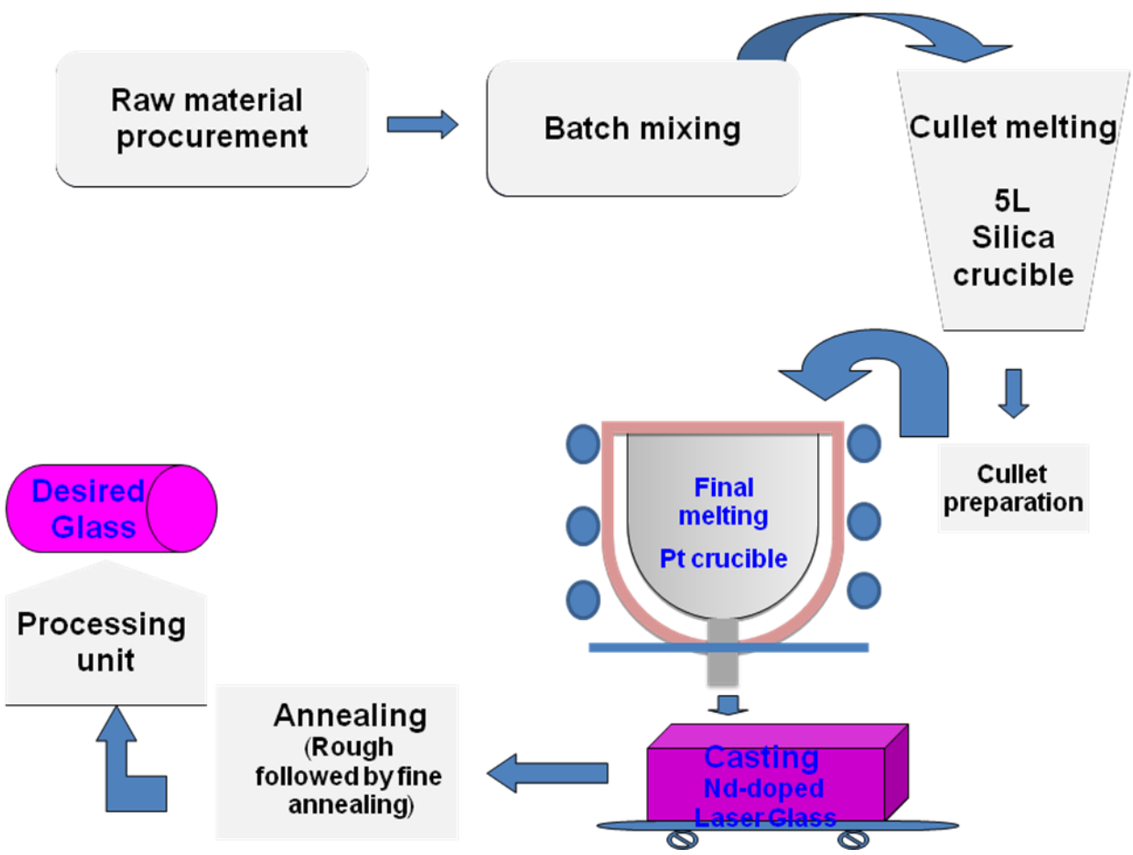

Fabrication of LASER glass rods

5 litre Pt bottom pouring crucible and induction furnace (at CGCRI)

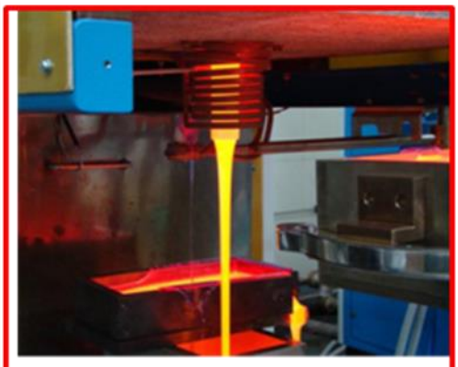

Casting of molten Nd:glass (at CGCRI)

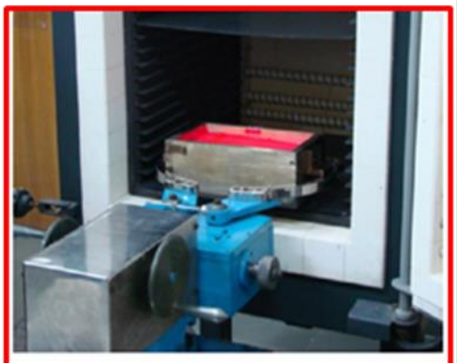

Transfer of cast glass to annealing furnace (at CGCRI)

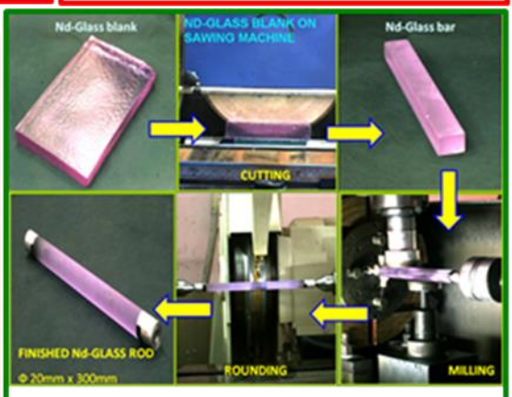

Machining and optical polishing of the Nd:glass rods (at RRCAT)

Optically polished Nd:glass slab & machined glass rod (at RRCAT)

Sol-gel spin coater (at RRCAT) holding a laser rod for AR coating

OH bond optimisation for the Indian glass

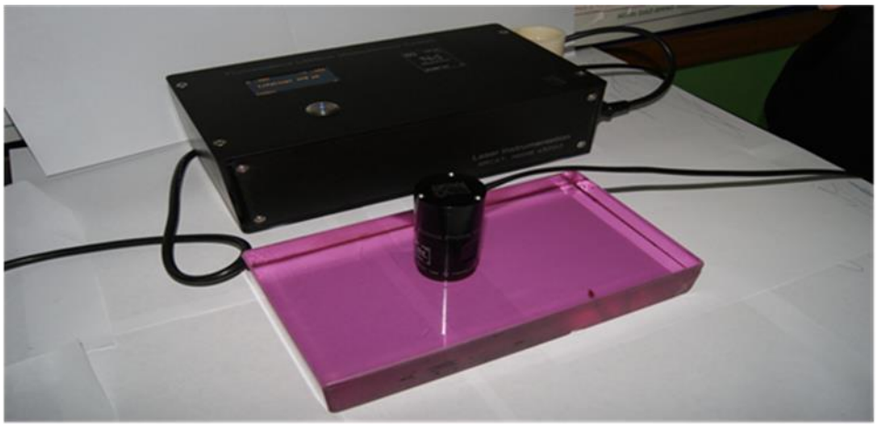

Fluorimeter developed at RRCAT

Characterization of Nd:phosphate glass

Fluorescence lifetime measurement for different OH concentrations

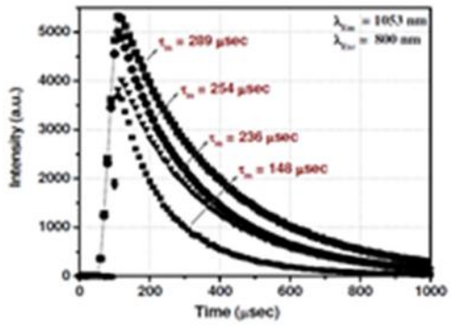

Life time vs OH bond concentration

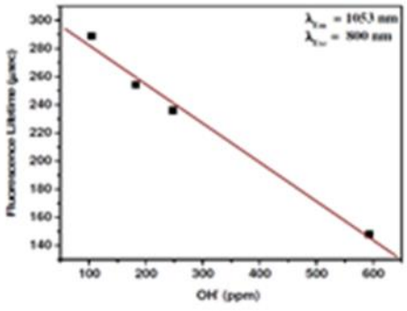

DIELECTRIC COATED OPTICS

- Dielectric coated (SiO_2 and HfO_2) coated optics
- Sol-gel coated optics (silica and zirconia/Titania/halfnia based sols)

Sol-gel coated optics preferred over dielectric coated optics because of low impurity content in coating materials